



Turun yliopisto  
University of Turku

# STRIATAL AND EXTRASTRIATAL DOPAMINE D<sub>2/3</sub> RECEPTORS STUDIED WITH [<sup>11</sup>C]RACLOPRIDE AND HIGH-RESOLUTION PET

---

Kati Alakurtti

## University of Turku

---

Faculty of Medicine  
Department of Clinical Physiology and Nuclear Medicine  
Turku PET Centre  
Turku Doctoral Program of Clinical Investigation  
Turku University Hospital and  
University of Turku, Turku, Finland

## Supervised by

---

Professor Juha O. Rinne  
Turku PET Centre  
Department of Neurology  
Turku University Hospital and  
University of Turku, Turku, Finland

## Reviewed by

---

Professor Jesper Ekelund  
Department of Psychiatry  
University of Helsinki  
Helsinki, Finland

Docent Esko Vanninen  
Kuopio University Hospital  
Science Service Center  
Kuopio, Finland

## Opponent

---

Professor Gitte Moos Knudsen  
Department of Neurology  
and Neurobiology Research Unit  
Copenhagen University Hospital  
Copenhagen, Denmark

The originality of this thesis has been checked in accordance with the University of Turku quality assurance system using the Turnitin OriginalityCheck service.

ISBN 978-951-29-6246-4 (PRINT)

ISBN 978-951-29-6247-1 (PDF)

ISSN 0355-9483

Painosalama Oy - Turku, Finland 2015

*to "Lucky"*

## ABSTRACT

Kati Alakurtti

### **Striatal and extrastriatal dopamine D<sub>2/3</sub> receptors studied with [<sup>11</sup>C]raclopride and high-resolution PET.**

Department of Clinical Physiology and Nuclear Medicine, Turku PET Centre, Turku Doctoral Program of Clinical Investigation, University of Turku, Turku University Hospital, Turku, Finland

The human striatum is a heterogeneous structure representing a major part of the dopamine (DA) system's basal ganglia input and output. Positron emission tomography (PET) is a powerful tool for imaging DA neurotransmission. However, PET measurements suffer from bias caused by the low spatial resolution, especially when imaging small, D<sub>2/3</sub>-rich structures such as the ventral striatum (VST). The brain dedicated high-resolution PET scanner, ECAT HRRT (Siemens Medical Solutions, Knoxville, TN, USA) has superior resolution capabilities than its predecessors. In the quantification of striatal D<sub>2/3</sub> binding, the *in vivo* highly selective D<sub>2/3</sub> antagonist [<sup>11</sup>C] raclopride is recognized as a well-validated tracer.

The aim of this thesis was to use a traditional test-retest setting to evaluate the feasibility of utilizing the HRRT scanner for exploring not only small brain regions such as the VST but also low density D<sub>2/3</sub> areas such as cortex. It was demonstrated that the measurement of striatal D<sub>2/3</sub> binding was very reliable, even when studying small brain structures or prolonging the scanning interval. Furthermore, the cortical test-retest parameters displayed good to moderate reproducibility. For the first time *in vivo*, it was revealed that there are significant divergent rostrocaudal gradients of [<sup>11</sup>C]raclopride binding in striatal subregions.

These results indicate that high-resolution [<sup>11</sup>C]raclopride PET is very reliable and its improved sensitivity means that it should be possible to detect the often very subtle changes occurring in DA transmission. Another major advantage is the possibility to measure simultaneously striatal and cortical areas. The divergent gradients of D<sub>2/3</sub> binding may have functional significance and the average distribution binding could serve as the basis for a future database.

**Key words:** dopamine, PET, HRRT, [<sup>11</sup>C]raclopride, striatum, VST, gradients, test-retest.

# TIIVISTELMÄ

Kati Alakurtti

## **Dopamiini D<sub>2/3</sub> reseptorien kuvantaminen korkean resoluution PET kameralla ja [<sup>11</sup>C]raclopridi merkkiaineella.**

Kliinisen Fysiologian ja Isotooppilääketieteen oppiaine, Valtakunnallinen PET-keskus, Turun Yliopisto, Turun Yliopistollinen Keskussairaala, Turku

Aivojen tyvitumakkeisiin kuuluva aivojuovio on keskeinen dopamiiniaineenvaihdunnan kannalta. PET menetelmällä voidaan tutkia dopamiiniaineenvaihduntaa reseptoritasolla, mutta sen heikkous on huono spatiaalinen resoluutio, etenkin tutkittaessa pieniä aivoalueita kuten aivojuovion ventraalista osaa (VST). Tässä väitöskirjatutkimuksessa on käytetty aivotutkimukseen suunniteltua korkean resoluution PET-kameraa (ECAT HRRT, Siemens Medical Solutions, Knoxville, TN, USA) ja D<sub>2/3</sub> dopamiinireseptoreihin spesifisesti sitoutuvaa [<sup>11</sup>C]raclopridi PET-merkkiainetta.

Tämän väitöskirjatutkimuksen tarkoituksena on selvittää toistomittauksella HRRT kameran soveltuvuutta pienten (VST) ja toisaalta vähän D<sub>2/3</sub> reseptoreita sisältävien (aivojen kuorikerros) aivoalueiden kuvantamiseen. HRRT-kameran käyttökelpoisuus osoittautui erittäin hyväksi pienempien aivoalueiden tutkimisessa eikä luotettavuus kärsinyt vaikka kahden mittauksen välistä intervallia pidennettiin. Kuorikerroksen mittauksen luotettavuus oli myös tyydyttävä/hyvä. Lisäksi ensimmäistä kertaa PET menetelmää käyttäen pystyttiin havaitsemaan erisuuntaisia gradientteja [<sup>11</sup>C]raclopridin sitoutumisessa D<sub>2/3</sub> reseptoreihin.

Löydösten perusteella korkean resoluution [<sup>11</sup>C]raclopridi PET menetelmä on erittäin luotettava ja se mahdollisesti lisää mittauksen sensitiivisyyttä havaita hienovaraisia dopamiiniaineenvaihdunnan muutoksia. [<sup>11</sup>C]raclopridia voisi tulevaisuudessa mahdollisesti käyttää samanaikaisesti sekä aivojuovion että aivojen kuorikerroksen tutkimiseen, joka toisi lisäinformaatiota dopamiinijärjestelmän toiminnallisesta järjestäytymisestä aivoissa. Havaituilla erilaisilla gradienteilla [<sup>11</sup>C]raclopridin sitoutumisessa voi olla funktionaalista merkitystä ja keskimääräistä sitoutumista voitaisiin käyttää myös tietokannan pohjana.

**Avainsanat:** dopamiini, PET, HRRT, [<sup>11</sup>C]raclopridi, aivojuovio, VST, toistomittaus

## TABLE OF CONTENTS

<b>ABSTRACT</b> .....	<b>4</b>
<b>TIIVISTELMÄ</b> .....	<b>5</b>
<b>ABBREVIATIONS</b> .....	<b>8</b>
<b>LIST OF ORIGINAL PUBLICATIONS</b> .....	<b>10</b>
<b>1. INTRODUCTION</b> .....	<b>11</b>
<b>2. REVIEW OF THE LITERATURE</b> .....	<b>12</b>
2.1 DOPAMINE SYSTEM .....	12
2.1.1 Major Dopaminergic Pathways .....	12
2.1.2 Basal Ganglia Circuitry .....	12
2.1.3 Dopamine Receptors .....	13
2.1.4 Pathology .....	14
2.2 PET IMAGING .....	15
2.2.1 Principles .....	15
2.2.2 ECAT HRRT PET Scanner .....	16
2.3 MEASUREMENT OF D <sub>2/3</sub> RECEPTORS .....	18
2.3.1 Modeling .....	18
2.3.2 Simplified Reference Tissue Model (SRTM) .....	19
2.3.3 D <sub>2/3</sub> Receptor Radioligands .....	21
2.3.4 Occupancy Model .....	21
2.3.5 Study Design .....	22
2.4 TEST-RETEST RELIABILITY OF [ <sup>11</sup> C]RACLOPRIDE BINDING .....	22
2.5 STRIATAL ORGANIZATION OF D <sub>2/3R</sub> IN NORMAL AGING AND BRAIN PATHOLOGY .....	23
<b>3. OBJECTIVES OF THE STUDY</b> .....	<b>25</b>
<b>4. SUBJECTS AND METHODS</b> .....	<b>26</b>
4.1 SUBJECTS .....	26
4.2 STUDY DESIGNS .....	26
4.3 PET METHODS .....	27
4.3.1 Radiochemistry .....	27
4.3.2 Image Acquisition .....	27
4.3.3 Image Preprocessing .....	28
4.3.4 Region of Interest Analysis .....	30
4.3.5 Quantification of [ <sup>11</sup> C]raclopride Binding .....	32
4.4 STATISTICAL ANALYSIS .....	32
4.5 MOTION DATA .....	33

---

<b>5. RESULTS</b> .....	<b>34</b>
5.1 REPRODUCIBILITY OF STRIATAL AND THALAMIC D2/3R BINDING (I) .....	34
5.2 LONG TERM TEST RETEST RELIABILITY OF STRIATAL AND EXTRASTRIATAL DOPAMINE D2/3R BINDING (II) .....	36
5.3 ROSTROCAUDAL GRADIENTS OF DOPAMINE D2/3R BINDING (III) .....	40
<b>6. DISCUSSION</b> .....	<b>42</b>
6.1 METHODOLOGICAL CONSIDERATIONS .....	42
6.2 HRRT PET AND EXPERIMENTAL SIGNAL PROCESSING (I) .....	43
6.3 TEST-RETEST RELIABILITY OF STRIATAL AND THALAMIC MEASUREMENTS (I, II) .....	45
6.4 TEST-RETEST RELIABILITY OF CORTICAL MEASUREMENTS (II) .....	46
6.5 ROSTROCAUDAL GRADIENTS OF D2/D3R BINDING (III) .....	48
<b>7. FUTURE DIRECTIONS</b> .....	<b>50</b>
<b>8. CONCLUSIONS</b> .....	<b>51</b>
<b>9. ACKNOWLEDGEMENTS</b> .....	<b>52</b>
<b>10. REFERENCES</b> .....	<b>54</b>
<b>ORIGINAL PUBLICATIONS</b> .....	<b>59</b>

## ABBREVIATIONS

AC	Anterior commissure
AUC	Area under the curve
AP	Anterior-posterior
$B_{\text{avail}}$	Receptor availability
BF	Basis function
B/I	Bolus plus infusion method
$B_{\text{max}}$	Receptor density
BP	Binding potential
$BP_{\text{ND}}$	Non-displaceable binding potential
COV	Coefficient of variation
D2/3R	Dopamine D2 and D3 receptors
DA	Dopamine
DAT	Dopamine transporter
DCA	Dorsal caudate nucleus
DLPFC	Dorsolateral prefrontal cortex
DOI	Depth of interaction
DPU	Dorsal putamen
ECAT	Emission computer aided tomography
$f_{\text{ND}}$	Free fraction in non-displaceable compartment
FOV	Field of view
GABA	Gamma aminobutyric acid
GPI	Globus pallidus internal
GPe	Globus pallidus external
HRRT	High-resolution research tomography
ICC	Intra-class correlation coefficient
$K_{\text{bol}}$	A bolus-to-infusion rate ratio
Kd	Equilibrium dissociation component
LOR	Line of response
LSO	Lutetium oxyorthosilicate



---

LYSO	Lutetium yttrium orthosilicate
MIP	Maximum intensity projection
MNI	Montreal Neurological Institute
MRI	Magnetic resonance imaging
MSA	Multiple system atrophy
MSN	Medium spiny neurons
NAcc	Nucleus Accumbens
NEC	Noise-equivalent count
OSEM	Ordinary Poisson-ordered subset expectation maximization
OFC	Orbitofrontal cortex
PET	Positron emission tomography
PD	Parkinson's disease
PSF	Point spread function
PSP	Progressive supranuclear palsy
PVE	Partial volume effect
R	Second-order regression analysis
r	Pearson correlation coefficient
$r_s$	non-parametric Spearman correlation coefficient
ROI	Region of interest
RM	Ratio method
SD	Standard deviation
SNc	Substantia nigra pars compacta
SNr	Substantia nigra pars reticulata
SPET	Single photon emission computed tomography
SPM	Statistical parametric mapping
SRTM	Simplified reference tissue model
STN	Subthalamic nucleus
TAC	Time-activity-curve
VAR	Variability
VST	Ventral striatum

## LIST OF ORIGINAL PUBLICATIONS

This thesis is based on the following original publications which are referred to in the text by the roman numbers of **I-III**:

- I** Alakurtti, Kati, Sargo Aalto, Jarkko J Johansson, Kjell Någren, Terhi Tuokkola, Vesa Oikonen, Matti Laine, ja Juha O Rinne. "Reproducibility of striatal and thalamic dopamine D2 receptor binding using [11C]raclopride with high-resolution positron emission tomography". *Journal of Cerebral Blood Flow and Metabolism* 2011;1:155–65.
- II** Alakurtti, Kati, Jarkko J. Johansson, Juho Joutsa, Matti Laine, Lars Bäckman, Lars Nyberg, ja Juha O. Rinne. "Long-Term Test-Retest Reliability of Striatal and Extrastriatal Dopamine D<sub>2/3</sub> Receptor Binding: Study with [(11)C]raclopride and High-Resolution PET". *Journal of Cerebral Blood Flow and Metabolism* 2015;doi:10.1038/jcbfm.2015.53.
- III** Alakurtti, Kati, Jarkko J Johansson, Terhi Tuokkola, Kjell Någren, ja Juha O Rinne. "Rostrocaudal Gradients of Dopamine D<sub>2/3</sub> Binding in Striatal Subregions Measured with [(11)C]raclopride and High-Resolution Positron Emission Tomography". *NeuroImage* 2013;82:252–59.

The original publications (**I-III**) have been reproduced with the permission of the copyright holders.

## 1. INTRODUCTION

Dopamine (DA) is one of the most important neurotransmitters in the brain. Many cognitive and motor functions rely on a normally functioning DA system and its impairment has been implicated in several well-known pathologies such as Parkinson's and schizophrenia. Dopamine  $D_{2/3}$  receptors are crucially involved in dopaminergic neurotransmission as many of its functions are mediated through these receptor subtypes.  $D_{2/3}$  receptors predominate mostly in the striatum which is a functionally and anatomically heterogeneous structure. The functional organization of the striatum derives from its cortical innervations. It is possible to detect imbalances in the striatal DA transmission via differences in the amount or in the distribution of the receptors in these functional subregions. Accordingly, the pathology is reflected in defects in either motor control or cognitive functions. Thus,  $D_{2/3}$  radiotracer positron emission tomography (PET) techniques have been developed to explore this phenomenon. The introduction of the high-resolution research PET scanner (HRRT) made it possible to visualize the DA system with higher accuracy than could be achieved with conventional whole body PET scanners. [ $^{11}\text{C}$ ]raclopride has been used to indirectly assess changes in the endogenous synaptic DA concentration in the striatum in response to drugs such as amphetamine and also after cognitive challenges. DA is thought to compete with [ $^{11}\text{C}$ ]raclopride for access to the  $D_{2/3}$  receptors and thus DA released in response to a challenge is reflected as a reduction in [ $^{11}\text{C}$ ]raclopride binding. Obviously, accurate and reproducible measurement of "baseline"  $D_{2/3}$  receptor availability is very important for such studies. The reproducibility of [ $^{11}\text{C}$ ]raclopride binding in human striatum has been demonstrated to be excellent in various test-retest studies, with different time intervals. However, as [ $^{11}\text{C}$ ]raclopride has only moderate affinity for the  $D_{2/3}$  receptors, it has been considered suboptimal in exploring regions in which there are low  $D_{2/3}$  receptors densities such as cortex. The connectivity of the DA system is an area of intense research and the possibility to study simultaneously both striatal and cortical DA transmission would be highly beneficial. When investigating the dopaminergic basis of human behavior and its role in disease mechanisms, it would be very advantageous to be able to reliably study substantially smaller DA release evoked by non-pharmacological stimuli. However, it is only possible to detect these subtle changes if the measurement methods being used are sufficiently sensitive. The HRRT scanner's superior resolution improves the sensitivity but it has also been associated with a lower signal-to-noise-ratio which can hamper the reliability of the measurement. The aim of this thesis was to validate, for the first time *in vivo*, the capabilities of high-resolution [ $^{11}\text{C}$ ]raclopride PET to assess functional changes not only in the striatum but also in many extrastriatal areas and to measure the gradient of the [ $^{11}\text{C}$ ]raclopride binding in the striatal subregions.

## 2. REVIEW OF THE LITERATURE

### 2.1 DOPAMINE SYSTEM

#### 2.1.1 Major Dopaminergic Pathways

Although it is more than 50 years ago since the physiological functions of 3-hydroxytyramine (dopamine) were discovered, this catecholaminergic neurotransmitter is still the focus of much research activity. Dopamine generally acts on neuronal circuitry by evoking a relatively slow modulation of the fast neurotransmission mediated by glutamate and gamma aminobutyric acid (GABA). Due to its modulatory role, dopaminergic pathways are significant in many areas of central nervous function. Four major dopaminergic pathways have been recognized in the mammalian brain; the nigrostriatal, mesolimbic, mesocortical and tuberoinfundibular systems originating from the dopamine-containing cells A9 (nigrostriatal), A10 (mesolimbic and mesocortical), and A8 (tuberoinfundibular). These neurons are critical in many CNS functions, including movement, affect, reward, attention, working memory, and learning (See review by Beaulieu and Gainetdinov 2011).

#### 2.1.2 Basal Ganglia Circuitry

A model of basal ganglia circuitry involves cortical-striato-pallido-thalamic-cortical loops with primary inputs into striatum (putamen and caudate) from cortical glutamatergic, thalamic glutamatergic, and nigral dopaminergic projections. Based on these loops, the striatum is divided into functional subregions. In primates, the motor striatum consists of the dorsolateral post commissural putamen and a dorsolateral region in the caudate nucleus which is innervated by the primary motor cortex, premotor cortex, supplementary motor area and post arcuate premotor area. The associative striatum comprises the putamen rostral to the anterior commissure as well as most of the head, body and tail of the caudate, receiving its input from associative areas of the cortex and from the prefrontal cortex. The limbic striatum includes the nucleus accumbens (NAcc) and the most ventral parts of both the caudate nucleus and putamen, receiving extensive innervations from limbic structures, such as the hippocampus and amygdala, as well as from prefrontal areas with limbic and autonomic functions, such as the orbitofrontal cortex and anterior cingulate (Joel and Weiner 2000; Haber et al. 2003). Two major pathways lead from the striatum to the main output nuclei in the basal ganglia: internal segment of the pallidum (GPi) and substantia nigra pars reticulata (SNr); 1) the direct pathway via inhibitory GABAergic neurons, and 2) the indirect pathway, which also contains inhibitory GABAergic

neurons to GPe (external segment of GP). From there, inhibitory neurons project to subthalamic nucleus (STN) and excitatory glutamatergic neurons project from STN to GPi/SNr. GPi/SNr send inhibitory GABAergic neurons to the thalamus that project via excitatory neurons to several cortical areas, including the premotor and motor regions. There are many published studies demonstrating that the direct pathway generates the desired movement, while the indirect pathway suppresses unwanted surrounding movement. The dopaminergic nigrostriatal input regulates the activity of these direct and indirect pathways. The nigrostriatal dopaminergic fibers terminate on the shafts of the dendritic spines of the medium spiny neurons and the cortical afferents terminate on the heads of spines, enabling dopamine modulation of the corticostriatal input (Parent & Hazrati 1995; Gerfen & Surmier 2011). Balance between the activity of the direct and indirect pathway is necessary for normal movement.

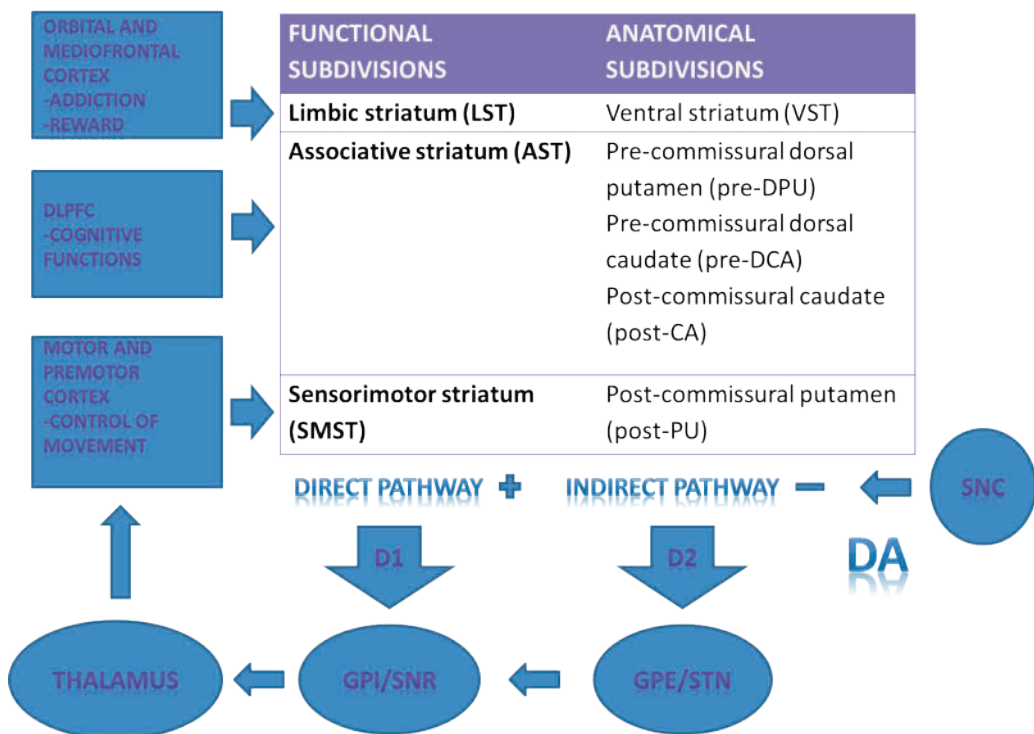


**Figure 1.** A schematic illustration of mechanisms for integrating information within the cortico-basal-ganglia circuitry. Regenerated from multiple sources (See for example Haber et al 2003).

### 2.1.3 Dopamine Receptors

The physiological actions of dopamine are mediated by five distinct but closely related G protein-coupled receptors that are divided into two major groups: the D1 type (D1 and D5) and the D2 type (D2, D3, D4) receptors. The subfamilies of D1- and D2-class receptors

are homogeneous with respect to their transmembrane domains but possess distinct pharmacological properties. D1-type dopamine receptors (D1 and D5) activate the  $G\alpha_{s/o}$  family of G proteins to stimulate cAMP production via adenylyl cyclase (AC); these are found exclusively post-synaptically on GABAergic medium spiny neurons (MSNs) in the striatum. The D2-type dopamine receptors (D2, D3, and D4) couple to the  $G\alpha_{i/o}$  family of G proteins and thus inhibit AC. Excitatory D1-like receptors are located exclusively in MSNs that project to the GPi/SNr (direct pathway), while inhibitory D2 receptors are located on post-synaptic neurons that project to GPe (indirect pathway). A small subpopulation of striatal MSN contains both D1- and D2-like receptors. However, D2 and D3 dopamine receptors are predominant both postsynaptically and presynaptically on dopaminergic neurons. Thus, the nigrostriatal fibers also express presynaptic D2 and D3 (autoreceptors); these are inhibitory receptors and their activation reduces dopamine release at the synaptic cleft between nigrostriatal fibers and MSNs (Gerfen and Surmier 2011; Beaulieu and Gainetdinov 2011).

The D1 receptor is the most widespread DA receptor and it displays the highest expression of any DA receptor. D1 mRNA has been found in the striatum, the Nacc and the olfactory tubercle. In addition, D1 receptors have also been detected in the limbic system, hypothalamus, and thalamus. The highest levels of D2 dopamine receptors are present in the striatum, the NAcc, and the olfactory tubercle but they are also expressed at significant levels in the substantia nigra, ventral tegmental area, hypothalamus, cortex, septum, amygdala, and hippocampus. The D3 dopamine receptor has its highest level of expression in the limbic areas, such as in the shell of the NAcc, the olfactory tubercle, and the islands of Calleja. Since dopamine is critically involved in a number of physiological processes, the different dopamine receptor subtypes have specific functional roles. D1, D2, and to a lesser degree D3, dopamine receptors have been the most extensively studied since they are critically involved in motor, learning, memory, reward and reinforcement mechanisms. In general, the specific physiological roles played by D3, D4, and D5 dopamine receptors in the brain are largely unknown. However, there is accumulating evidence that D3 dopamine receptors exert some modulatory influences on many of the functions generally attributed to D2 dopamine receptors and the role of the D3 receptor in addictive disorders is a topic of active research (See review by Missale et al. 1998; Gerfen and Surmier 2011).

#### 2.1.4 Pathology

Since dopamine is critically involved in a variety of functions, it is not surprising that multiple disorders have been related to dopaminergic dysfunctions. The best recognized is Parkinson's disease (PD) which is characterized by a degeneration of the nigrostriatal dopaminergic system with neuronal loss and reactive gliosis in the substantia nigra. Because the nigrostriatal pathway excites the direct pathway and

inhibits the indirect pathway, the loss of this input tips the balance in favor of activity in the indirect pathway leading to poverty of movements (DeLong 1983; Dickinson 2012). There are also several other neurodegenerative diseases affecting the DA system such as multiple system atrophy (MSA), progressive supranuclear palsy (PSP), Huntington's disease and dementia with Lewy bodies (Brücke et al. 1997; Antonini et al. 1997; Brooks 1998; Pavese et al. 2003). The DA system is also thought to be involved in many psychiatric disorders, although here the evidence is more indirect i.e. almost all of the clinically effective antipsychotics block D2 dopamine receptors, thus dopaminergic dysfunction has been associated with schizophrenia (Meisenzahl 2007; Guillin et al. 2007). Dopamine dysregulation has been speculated to occur in ADHD and Tourette's syndrome (Wong et al 2008; Volkow et al. 2011). The abnormalities in the reward mechanisms associated with drug abuse and addiction strongly suggest that dopamine also plays an important role in substance use conditions (Pierce and Kumaresan 2006; Volkow et al. 2011). A role for abnormal dopaminergic signaling has also been postulated in a host of other brain disorders, such as bipolar disorder and major depression (Suhara et al. 1992; Camardese et al 2014).

## 2.2 PET IMAGING

### 2.2.1 Principles

Positron emission tomography (PET) is a functional imaging technique that produces a three-dimensional image of biochemical and physiological processes in the brain. The system utilizes short lived radioactive isotopes, such as Oxygen-15, Carbon-11 and Fluoride-18 (half-lives of 2.1, 20.4 and 110 minutes, respectively), which are produced in a cyclotron, since these unstable positron emitters are not found in nature. The radionuclide (tracer), which is introduced into the body after being incorporated into a biologically active molecule of interest, undergoes radioactive decay and a scanner detects that radioactivity. As the radioisotope undergoes positron emission decay, it emits a positron that travels in tissue only for a short distance (for Carbon-11 the distance is about 0.85 mm), during which time it loses kinetic energy to a point where it can interact with an electron. The encounter annihilates both the electron and the positron, producing a pair of 511 keV (kiloelectron volt) annihilation (gamma) photons moving in approximately opposite ( $\sim 180.25^\circ$ ) directions. The coincidental detection of two photons on the opposite sides of the detector ring represents a true count. All of these coincident events occurring somewhere in the LOR (LOR=line of response = line between the two detections) during a time frame are collected and the PET image is reconstructed based on the temporal and spatial distribution of these events (Turkington 2001).

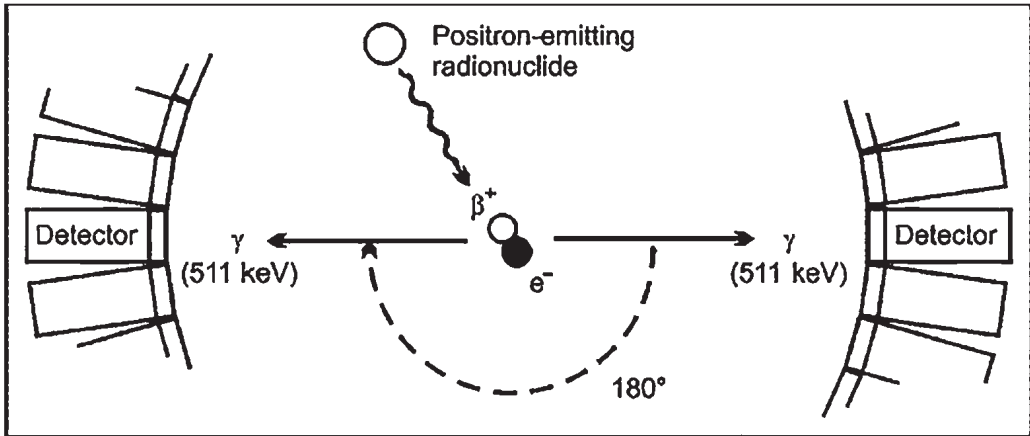


**Figure 2.** A schematic illustration of a coincidental detection of two photons inside the PET scanner. During the decay of the radionuclide, a positron is emitted and collides with an electron. The positron and electron annihilate each other, converting mass into 2 511-keV gamma quanta emitted at  $180^\circ$  to each other. Two annihilation photons are electronically detected as a coincidence event when they strike detectors simultaneously. Adopted from (Verel et al. 2005).

### 2.2.2 ECAT HRRT PET Scanner

The high resolution research tomograph, ECAT HRRT (Siemens Medical Solutions, Knoxville, TN, USA) is one of the most complex existing PET scanners. It is the only human size scanner with an axial resolution of about 2.5 mm full-width half maximum at the center of field of view (FOV). The scanner's gantry is surrounded by eight detector heads. Each detector is layered with two 1 cm thick detector layers of cerium-doped lutetium oxyorthosilicate (LSO) and cerium-doped lutetium-yttrium oxyorthosilicate (LYSO) crystals with decay times of 43-44 ns and 53 ns, respectively. The different decay times of the crystals make it possible to conduct a depth of interaction (DOI) determination to obtain a pulse shape discrimination. The crystals act as scintillators, absorbing the high radiation energy and converting it into light. The FOV of the dedicated brain scanner is 25 cm in the axial and 35 cm in the trans-axial direction, which means that the resulting slice thickness is 1.22 mm. In order to correct for tissue attenuation, transmission scans are performed with a  $^{137}\text{Cs}$  point source (662 keV  $\gamma$ -emitter,  $T_{1/2}=30.2\text{a}$ ) before each scan. Data is collected in 3-dimensions meaning that all possible LORs are included, thus increasing the sensitivity and resolution of the scanner. There are a photomultiplier tubes situated behind each detector and these transform scintillations into the electrical pulses that are recorded by the scanner system (Comtat et al. 2004; Sossi et al. 2005; De Jong et al 2007).





Figure 3. HRRT scanner in Turku PET-Centre (Photo by the author).

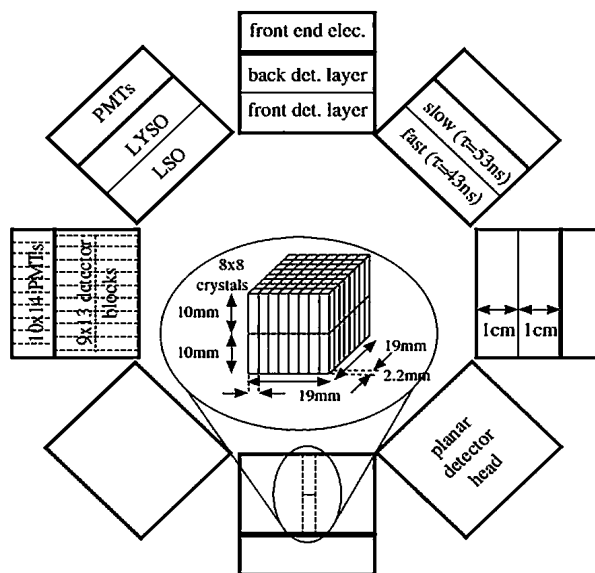
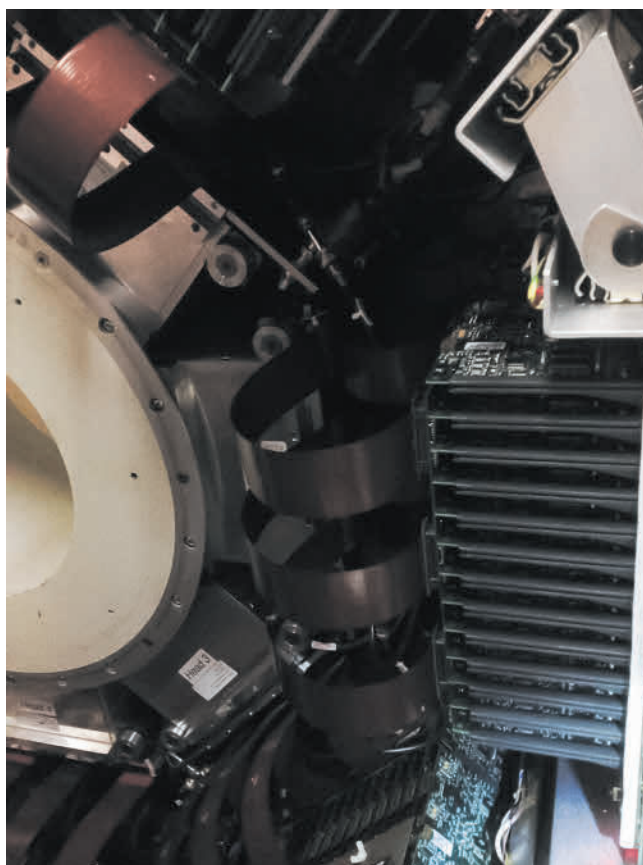


Figure 4. A Schematic illustration of detector arrangement in the ECAT HRRT. Adopted from (Sossi et al 2005).

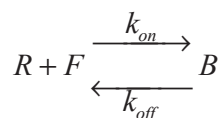


**Figure 5.** Detector head of HRRT scanner (Photo by the author)

## 2.3 MEASUREMENT OF $D_{2/3}$ RECEPTORS

### 2.3.1 Modeling

Imaging receptors kinetics with PET is based on prior decades of research using *in vitro* radioligand techniques. The basis for these *in vitro* experiments is the equilibrium binding reaction between receptors R and free ligand F in the formation of the bound ligand–receptor complex B, with reaction rate constants  $k_{on}$  and  $k_{off}$ .



The term ‘binding potential’ (BP) was based on *in vitro* radioligand binding. The concept was based on the linear role of two parameters (receptor density and radioligand affinity) to determine the amount of radioligand uptake in brain. Specifically, binding potential is defined as the ratio of  $B_{max}$  (receptor density) to  $K_D = k_{on}/k_{off}$  (radioligand equilibrium

dissociation constant). Because affinity of ligand binding is the inverse of  $K_D$ , ( $1/K_D$ ),  $BP$  can be viewed as the product of  $B_{\max}$  and affinity.

$$BP = \frac{B_{\max}}{K_D} = B_{\max} \times \frac{1}{K_D} = B_{\max} \times \text{affinity}$$

In PET studies, compartmental kinetic models describe the concentrations of the radiotracer in different physiological compartments (such as plasma, free and non-specifically bound and specifically bound compartments) and the rate constants of radiotracer transfer between these compartments to give estimates of radiotracer BP (Mintun et al. 1984).

*In vivo*, BP reflects the equilibrium concentration of specific binding as a ratio to some other reference concentration:

$BP_F$  is the ratio at equilibrium of the concentration of specifically bound radioligand in tissue to the concentration of free radioligand in tissue, which is assumed to equal the free concentration in plasma.

$BP_P$  is the ratio at equilibrium of specifically bound radioligand to that of total parent radioligand in plasma (free plus protein bound, excluding radioactive metabolites).

$BP_{ND}$  is the ratio at equilibrium of specifically bound radioligand to that of nondisplaceable radioligand in tissue (free and non-specifically bound).  $BP_{ND}$  is the typical measurement from reference tissue methods, as it compares the concentration of radioligand in receptor-rich to receptor-free regions. Thus, it is necessary to compare specific binding to *non-displaceable* binding in order to obtain the parameter  $BP_{ND}$ .

$$BP_{ND} = f_{ND} \frac{B_{\text{avail}}}{K_D}$$

Where  $B_{\text{avail}}$  is the receptor density (available for binding),  $1/K_D$  is the affinity and  $f_{ND}$  is the free fraction of radiotracer in the non-displaceable tissue compartment. The parameter  $f_{ND}$  is usually assumed to be equal in receptor-rich and receptor-free regions, assuming that nonspecific binding is the same in both areas (Innis et al. 2007).

### 2.3.2 Simplified Reference Tissue Model (SRTM)

In dynamic PET studies, an input function (arterial plasma concentration) describing the time course of the delivery of the radiotracer to the tissue is required for quantification, but to avoid the need for arterial sampling, the plasma input function may be substituted by using a reference region. The reference tissue model needs the presence of a reference tissue i.e. a region in which there is no specific binding of the ligand in order to estimate non-displaceable uptake of the ligand. The time course of radioligand uptake in the tissue of interest is expressed in terms of its uptake in the reference tissue, with the assumption that

the level of nonspecific binding will be the same in both tissues. This model assumes that the exchange between free and nonspecific binding has to be fast enough so that they can be considered as one compartment. The advantage of the reference tissue method is clear as no arterial cannulation and blood sampling are required, reducing the degree of invasiveness and the level of complexity of both the scanning protocol and the data analysis procedures (Lammertsma and Hume 1996). With [ $^{11}\text{C}$ ]raclopride, the cerebellum may be used as a reference region since it is devoid of D2/3R (Gunn et al. 1997; Lammertsma and Hume, 1996).

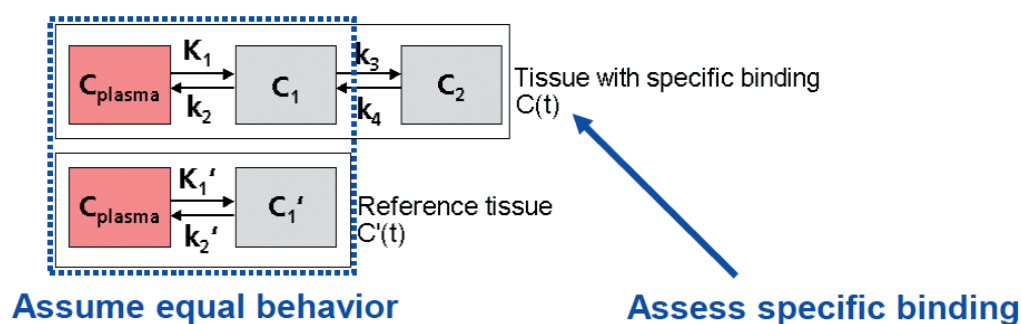


**Figure 6.** A schematic presentation of the two-tissue compartmental model, from which the reference tissue model (SRTM) is derived.  $C_{\text{plasma}}$  = Concentration of the ligand in plasma;  $C_1$  and  $C_1'$  = Concentration of non-displaceable ligand in the tissue (free + nonspecifically bound ligand);  $C_2$  = Concentration of specifically bound ligand in the tissue;  $K_1$  and  $K_1'$  = Rate constant for transfer from plasma to non-displaceable compartment;  $k_2$  and  $k_2'$  = Rate constant for transfer from the non-displaceable compartment to plasma;  $k_3$  = Rate constant for transfer from the non-displaceable compartment to the specifically bound compartment;  $k_4$  = Rate constant for transfer from the bound to the non-displaceable compartment. This figure has been depicted in several sources in the literature (See for example, Laruelle 2000).

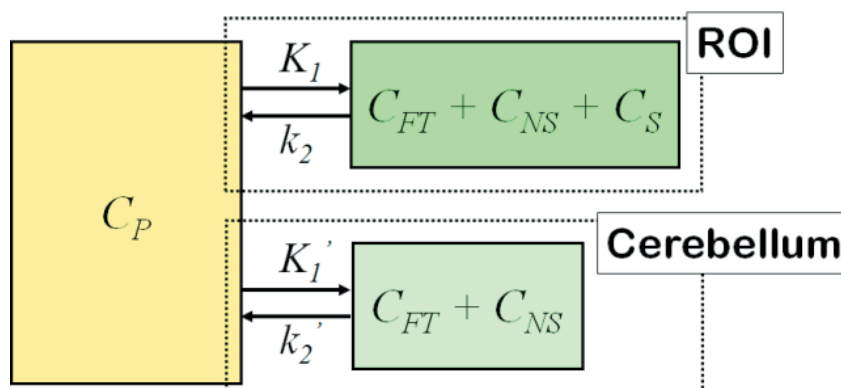


**Figure 7.** SRTM can be used when one-tissue compartmental model could reasonably describe the kinetics of the tracer that is, in the target tissue the free and nonspecifically bound ligand cannot be kinetically distinguished from the specifically bound.  $C_P$  = concentration of the ligand in plasma;  $C_{FT}$  = concentration of free ligand in tissue;  $C_{NS}$  = concentration of nonspecifically bound in the tissue;  $C_S$  = concentration of the specifically bound ligand in the tissue.  $K_1$  and  $K_1'$  = Rate constant for transfer from plasma to tissue compartment;  $k_2$  and  $k_2'$  = Rate constant for transfer from the tissue compartment to plasma; ROI = region of interest. (Illustration is by courtesy of Vesa Oikonen).

### 2.3.3 D<sub>2/3</sub> Receptor Radioligands

In vitro studies of D2 receptors reveal the existence of high (D2<sup>high</sup>) and low (D2<sup>low</sup>) affinity states and the D2<sup>high</sup> state is regarded as the functional state due to G-protein coupling. Whilst antagonists have equal affinity at both receptor states, agonists have greater affinity for the D2<sup>high</sup> (1–10 nM) than the D2<sup>low</sup> state (0.7–1.5 mM). D<sub>2/3</sub> receptor binding in the striatum is generally quantified using either the gold standard PET radioligand [<sup>11</sup>C]raclopride, or the single photon emission tomography (SPET) radioligands [<sup>123</sup>I]IBZM and [<sup>123</sup>I]epidepride. (See review by Egerton et al. 2009). The recently developed D<sub>2/3</sub> agonist radiotracers such as [<sup>11</sup>C]PHNO and [<sup>11</sup>C]NPA have higher affinity for the D3 receptors over D2 receptors and also for the D2<sup>high</sup> receptors (Narendran et al. 2004; Shotbolt et al. 2012). In order to measure extrastriatal D<sub>2/3</sub> receptor availability and possible DA release, high affinity antagonist radiotracers such as [<sup>11</sup>C]FLB457 and [<sup>18</sup>F]fallypride are required (Slifstein et al. 2004; Narendran et al. 2009). [<sup>11</sup>C]raclopride, a substituted benzamide, has an equal and relatively low affinity for the dopamine D2 and D3 receptors (from now on denoted as D2/3R) making it optimal to compete with endogenous dopamine (Seeman et al. 1989; Logan et al. 1991; Young et al. 1991). It is a highly selective D2/3R antagonist and widely-used in PET studies assessing D2/3R availability. [<sup>11</sup>C]raclopride dissociates sufficiently rapidly from receptors, allowing binding equilibrium to be established *in vivo* within the time span of a PET experiment (Farde et al. 1985; Hall et al. 1988).

### 2.3.4 Occupancy Model

Detecting endogenous transmitter release, in this case DA, is based on the estimation of changes in the concentration of available neuro-receptor binding sites ( $B_{avail}$ ), which occur in response to the changes in the local neurotransmitter concentration according to the Michaelis–Menten equation. The kinetic behavior of the radioligand, in this case [<sup>11</sup>C]raclopride, is in turn dependent on  $B_{avail}$ , and is linear at tracer concentrations. The observed changes in  $BP_{ND}$  are usually presumed to reflect changes in  $B_{avail}$ , rather than in the KD. Based on the “classical occupancy model”, D2/3R radiotracers compete with DA for receptor binding, thus a decrease in  $BP_{ND}$  is assumed to reflect increased DA release. (Laruelle, 2000). For example, decreases in binding of [<sup>11</sup>C]raclopride to dopamine D2/3R has been detected following administration of the DA re-uptake inhibitor methylphenidate (Volkow et al. 1994). These techniques using different pharmacological challenges have helped clarify the neuropharmacology of DA release in the human brain and have revealed novel details of the neurochemistry of many brain disorders (Dewey et al. 1993; Breier et al. 1998; Piccini et al. 2003). The ability to study DA release produced by non-pharmacological stimuli is also of interest providing information about the dopaminergic basis of human behavior and its role in disease mechanisms (Bäckman et al. 2011; Jonasson et al. 2014)

### 2.3.5 Study Design

Striatal DA release is most commonly investigated with approach, where two conditions, challenge and control, are used to infer the changes in DA release. In the challenge scan, the changes in D2/3R occupancy are induced before radiotracer administration (Laruelle, 2000). Scans are typically performed during the same day and [<sup>11</sup>C]raclopride is usually administered as a single bolus. In addition, [<sup>11</sup>C]raclopride may also be administered as an initial bolus followed by constant infusion (termed as the bolus plus infusion (B/I) method) where both control and activation data are collected within a single scan session (Carson et al. 1997; Watabe et al. 2000). In addition to simplicity, the B/I method has many advantages over the single bolus dual-scan approach as the measurements of D2/3R availability can be obtained under sustained binding equilibrium conditions. Once a state of equilibrium has been established, there is no net transfer of the radiotracer in or out of the brain and BP may be calculated as the ratio of the concentration of the radiotracer in the ROI to the concentration of the radiotracer in the reference region: ( $BP_{ND} = (CROI-CREF)/CREF$ ) (Watabe et al. 2000; Mawlawi et al. 2001; Martinez et al. 2003). However, the single B/I protocol can be problematic as it takes a rather long time for [<sup>11</sup>C]raclopride to reach equilibrium, which means that the post-challenge measurement has to be performed after there has been considerable decay of the isotope. In the dual B/I protocol, subjects are scanned twice, first at baseline and then during an intervention to provide a more reliable statistical evaluation (Martinez et al. 2003). This is a major advantage when measuring small brain regions such as VST and caudate nucleus or regions with lower densities of D2/3R such as cortical areas where adequate count rate statistics is essential.

## 2.4 TEST-RETEST RELIABILITY OF [<sup>11</sup>C]RACLOPRIDE BINDING

As described earlier, [<sup>11</sup>C]raclopride has been used to indirectly measure changes in endogenous synaptic DA concentration in the striatum in response to drugs such as amphetamine or cocaine (Drevets et al. 1999; Martinez et al. 2007) and also in response to cognitive challenges (Bäckman et al. 2011). DA is thought to compete with [<sup>11</sup>C]raclopride at D2/3R, and DA release during a challenge is reflected as a reduction in the extent of [<sup>11</sup>C]raclopride binding (Laruelle 2000). Obviously, accurate and reproducible measurement of “baseline” D2/3R availability is very important for these kinds of studies. The reproducibility of a single bolus of [<sup>11</sup>C]raclopride binding in human striatum has been evaluated in several studies using different time intervals (Hietala et al. 1999; Mawlawi et al. 2001; Hirvonen et al. 2003). In the early studies, the striatum was evaluated as a whole structure (Hietala et al 1999) and later subdivided into the putamen and caudate nucleus. Mawlawi and colleagues (2001) were the first group to measure VST separately. Most experiments have examined short-term test-retest reliability with scans carried out within 24 hours. There is one study on long-term stability of [<sup>11</sup>C]raclopride binding,

where two sets of scan pairs (intervals of 3 to 7 weeks and 6 to 11 months) were used (Hietala et al. 1999). The previous test-retest studies have demonstrated the test-retest reliability of striatal [ $^{11}\text{C}$ ]raclopride binding to be very good.

The amount of D2/3R in extrastriatal areas is only 2%–8% of that in the striatum (Suhara et al. 1999). Since [ $^{11}\text{C}$ ] raclopride has rather moderate *in vivo* affinity and a relatively low signal-to-noise ratio (affinity compared to nonspecific binding) in areas where D2/3R density is low, such as the cortex, [ $^{11}\text{C}$ ]raclopride is not optimal to quantify D2/3R availability in those areas (Farde et al. 1988). After the introduction of high-affinity radioligands such as [ $^{11}\text{C}$ ]FLB 457 and [ $^{18}\text{F}$ ]fallypride, it has been possible to quantify also extrastriatal D2/3R s (Halldin et al. 1995; Olsson et al 2004). With these high-affinity ligands, cortical test-retest reliability has been reported to be ~10% for [ $^{18}\text{F}$ ]fallypride and between 5.3% to 10.4% for [ $^{11}\text{C}$ ]FLB 457 (Mukherjee et al. 2002; Vilkmán et al. 2000). Although [ $^{11}\text{C}$ ] raclopride is suboptimal in the measurement of extrastriatal DA transmission, decreases in [ $^{11}\text{C}$ ]raclopride  $\text{BP}_{\text{ND}}$  have been observed in extrastriatal regions following drug or behavioral challenges (Piccini et al. 2003; Sawamoto et al. 2008; Stokes et al. 2010). Changes in extrastriatal [ $^{11}\text{C}$ ]raclopride binding have also been associated with brain pathology, such as that associated with Alzheimer's, Huntington's and Parkinson's diseases (Joyce et al. 1998; Ribeiro et al. 2009; Politis et al. 2011). In an earlier test-retest study conducted by Hirvonen et al. (2003), the attempts to describe [ $^{11}\text{C}$ ]raclopride binding consistently in temporal cortex failed since the specific signal was too low to detect accurately. Stokes et al. (2010) measured the cortical [ $^{11}\text{C}$ ]raclopride binding from a separate cohort of subjects (controls) where  $\Delta^9$ -tetrahydrocannabinol (THC) was administered to quantify possible alterations of DA transmission in the human cortex. ROI analyses including right middle frontal gyrus, left superior frontal gyrus and left superior temporal gyrus yielded relatively poor test-retest values with VAR values ranging from 18% to 24%.

## 2.5 STRIATAL ORGANIZATION OF D2/3R IN NORMAL AGING AND BRAIN PATHOLOGY

Previous post-mortem studies in humans have reported that the distribution of striatal D2/3R is uniform, both dorsoventrally and lateromedially (Hall et al. 1994; Piggott et al. 1999), whereas a rostrocaudally increasing gradient was detected in both the caudate nucleus and putamen (Piggott et al. 1999). These findings were soon reinforced by the *in vivo* results of pigs and monkeys (Rosa-Neto et al. 2004). Since the striatum is connected to cortical areas via specific dopaminergic pathways which contain receptor subtypes, the disturbances in cognitive and motor performance in pathological states become manifested characteristically within this topography (Bäckman et al. 2000; DeLong 1983; Evarts and Wise 1984; Kaasinen and Rinne 2002). Substriatal impairment of the DA system is present in several neurodegenerative diseases such as PD, MSA, progressive supranuclear palsy

(PSP), Huntington's disease and dementia with Lewy bodies (Antonini et al. 1997; Brücke et al. 1997; Kish et al. 1988; Rinne et al. 1991). The well-known pathology involving PD involves the degeneration of the dopaminergic neurones that provide an input primarily to the posterior sensorimotor striatum, which then results in the characteristic PD motor symptoms that are paralleled by cognitive deficits, particularly in executive function (Kaasinen and Rinne 2002; Nieoullon 2002). Although the striatal D2/3R are rather well preserved in early PD, decreased binding can be observed in MSA and PSP (Antonini et al. 1997; Brooks et al. 1992; Ghaemi et al. 2002). PET research has also demonstrated that in addition to detecting changes in the dopamine receptor density, it is also able to reveal distinctive changes in DA release in the subregions of the striatum (Mawlawi et al. 2001; Martinez et al. 2003). For example in individuals who experienced an intravenous administration of methylphenidate as pleasurable, there were lower striatal D2/3R levels whereas subjects who disliked the drug's effects exhibited higher D2/3R levels. Thus, a low density of D2/3R may be associated with psychostimulant abuse i.e. the hedonistic response to a drug predominates (Volkow et al. 1999). An imbalance in the DA system is also well-known component of schizophrenia. There is recent evidence suggesting that the nigrostriatal pathway has the highest dysregulation, a finding in contrast with the traditional view that most of the striatal DA hyperactivity involves the mesolimbic pathway. Moreover, there is also evidence that an excess of DA may be present in the prodromal phase of schizophrenia, which is itself an early pathogenic condition that eventually leads to irreversible cortical dysfunction (Kuepper et al. 2012).

Numerous studies have reported that striatal DA function decreases from early to late adulthood by 6%–10% per decade (Antonini and Leenders 1993; Rinne et al. 1993; Seeman et al. 1987; Volkow et al. 1998). It has also been postulated that D2/3R binding in the posterior putamen decreases significantly more with age than in the VST, indicating that there could well be distinct regional differences in the age-related changes in D2/3R binding (Kim et al. 2011). Thus, one would predict that it may be possible to detect age-related changes in D2/3R gradients in the distinct subregions of the striatum. The relationship between age-related DA changes and age-related cognitive changes has also been explored; it was found that there was a decrease in D2/3R binding with advancing age with a negative relationship between age and performance in cognitive tests. In addition, a moderate to strong relationship between D2/3 binding and motor and cognitive performance has been detected even after controlling for chronological age, indicating that DA activity may influence performance irrespective of age (Bäckman et al. 2000; Volkow et al. 1998). Age-related decreases in dopamine D2/3R availability have also been associated with neuropsychological test performance involving frontal brain regions and in cocaine abusers with reduced metabolism in the frontal regions of the brain (Volkow et al. 1993b, 1998).



### 3. OBJECTIVES OF THE STUDY

The aim of studies **I** and **II** was to validate the use of high-resolution [<sup>11</sup>C]raclopride PET in studying not only substriatal but also extrastriatal DA transmission. In study **III**, the aim was to exploit the HRRT's superior resolution to try to detect the rostrocaudal gradients of [<sup>11</sup>C]raclopride binding in the striatal subregions.

The specific aims of these studies were

- To evaluate with the traditional single bolus of [<sup>11</sup>C]raclopride test-retest setting, the feasibility of exploiting the HRRT scanner to explore small brain regions such as the VST and to devise experimental signal processing methods to determine whether the scanner's high-resolution features would hamper the reliability of the measurement (**I**).
- To investigate the long-term stability of the D2/3R binding and to examine whether [<sup>11</sup>C]raclopride could be used in measuring also extrastriatal DA transmission using the B/I technique in a test-retest setting with five weeks' interval (**II**).
- To detect, for the first time *in vivo*, rostrocaudal gradients in D2/3R binding in the distinct striatal subregions.

## 4. SUBJECTS AND METHODS

### 4.1 SUBJECTS

Studies included a total number of 14 subjects and 28 [ $^{11}\text{C}$ ]raclopride PET scans. All studied subjects were right-handed, non-smoking male volunteers free of any somatic or psychiatric illness. All study protocols were reviewed and approved by the Ethics Committee of the Hospital District of Southwestern Finland. Subjects were given written information about all essential issues involved in the study. Written consent was obtained from each volunteer. All studies were carried out according to the ethical guidelines given by the Declaration of Helsinki.

In studies **I** and **III**, seven subjects were recruited, interviewed and physically screened. All subjects underwent 1.5 T magnetic resonance (MR) imaging to obtain an anatomical reference and to exclude any brain pathology. The age, height, and weight of the subjects were  $24.5 \pm 3.5$  years,  $185.5 \pm 12.5$  cm, and  $74 \pm 14$  kg, respectively (mean  $\pm$  s.d.).

In study **II**, seven male university students took part in an ongoing trial on the effects of working-memory training on striatal dopamine release. These seven subjects were from the control group and received no training, and they were chosen for the test-retest analyses based on optimal motion data (See section 4.5 Motion Data for details). To rule out any structural brain abnormalities and to obtain anatomical references, all subjects underwent 3T magnetic resonance imaging. Age, height, and weight of the subjects were  $24 \pm 2$  years,  $176 \pm 1$  cm, and  $69 \pm 3$  kg, respectively (mean  $\pm$  s.d.).

### 4.2 STUDY DESIGNS

Study **I** set out to evaluate the test-retest reliability of the striatal and thalamic dopamine D2/3R binding using single bolus [ $^{11}\text{C}$ ]raclopride and the high-resolution research tomograph (HRRT). Subjects ( $n=7$ ) were scanned twice during the same day with a 2.5 hour interval, in the resting state. VST was analyzed separately in order to evaluate whether HRRT could be utilized to explore such a small anatomic structure. However, HRRT scanner's superior spatial resolution has been associated with a lower signal-to-noise ratio potentially hampering the measurement. Different experimental signal processing methods were examined to explore this issue. Conventionally, in the histogram mode image reconstruction, discrete time points are fixed in the sinogram space while counting statistics are allowed to vary. This originates from working with old generation scanners that were not able to record all events as a stream in the acquisition disk. Modern scanners, such as the HRRT, are able to record all events in a so-called list

mode format, which allows the operators to determine framing after scanning. Thus, a new set of sinograms with more homogeneous noise characteristics was created.

Study II evaluated the long-term test–retest reliability of [<sup>11</sup>C]raclopride binding in striatal subregions, the thalamus and the cortex using the bolus-plus-infusion method and an HRRT scanner. Subjects (n=7) underwent two PET scans while performing a simple computerized working memory task, five weeks apart.

Study III measured the rostrocaudal gradients of [<sup>11</sup>C]raclopride binding to dopamine D2/3R in the striatum using the HRRT scanner. Data of the retest scan from the same subjects (n=7) used in the previous test-retest study was reanalyzed and the mean BP<sub>ND</sub> was sampled plane-by-plane, 1.5mm apart, on spatially normalized parametric images of each substriatal region.

## 4.3 PET METHODS

### 4.3.1 Radiochemistry

A detailed description of the preparation of [<sup>11</sup>C]raclopride is given in paper I. There were no statistically significant differences to be found in the specific radioactivities, in the injected doses, or in the injected masses between the test and the retest scans. However, in study I, one outlier (injected mass of 13.03  $\mu$ g) was detected in the boxplot analysis. Although the injected mass was above the average, it was considered tolerable with regard to pharmacological effects and thus the subject was not excluded from the final analysis. Radiochemical purity was over 99.5% in all studied cases.

### 4.3.2 Image Acquisition

PET experiments were carried out using a brain-dedicated high-resolution PET scanner, the ECAT high-resolution positron emission scanner (HRRT; Siemens Medical Solutions, Knoxville, TN, USA). The HRRT is a dual-layer, crystal-detector scanner which makes a depth-of-interaction measurement for coincident photons. It is characterized by an isotropic 2.5-mm intrinsic spatial resolution. The spatial resolution in the reconstructed images varies in the radial and tangential directions from about 2.5 to ~3 mm and in the axial directions from 2.5 to 3.5 mm in the 10-cm field of view covering most of the brain. In order to minimize the head movement, an individually shaped thermoplastic mask was used with each subject and an external position detector (Polaris Vicra, Northern Digital, Waterloo, Ontario, Canada) was used to monitor the head movement. Before each emission scan started, a transmission scan was performed using a <sup>137</sup>Cs point source. To further verify that the subject's head was positioned in the retest scan in the same way as in the first scan, two laser beams were aligned with sagittal and orbitomeatal lines on the face and these were marked on the mask with ink.

In study **I**, the subject's left antecubital vein was cannulated and a single bolus of [ $^{11}\text{C}$ ]raclopride bolus was injected intravenously and flushed with saline. Subjects underwent two PET scans with a 2.5 hours' interval in the resting state. The emission scan started at the time of injection and data were collected for 55 minutes in the list mode format.

In study **II**, the left antecubital vein was cannulated and intravenous [ $^{11}\text{C}$ ]raclopride bolus injections were administered directly followed by a continuous infusion of [ $^{11}\text{C}$ ]raclopride for 80 minutes. A bolus-to-infusion rate ratio ( $K_{\text{bol}}$ ) of 105 minutes and a bolus component of 50% (of the total volume of the tracer) were chosen according to previous publications (Watabe et al 2000; Mawlawi et al. 2001). Each subject underwent two [ $^{11}\text{C}$ ]raclopride PET scans, 5 weeks apart. Each scan started with 55 minutes of baseline measurement during which the subjects performed a very simple computerized letter-recall task, followed by a 25 minutes' working memory task. Only the first 55 minutes of acquisition data were used in the test-retest analyses. During the baseline acquisition, the subjects were shown 7 to 15 letter sequences, where all the letters were identical (e.g., A – A – A – ...). When the letter sequence ended, the subjects were asked to report the last four letters that were shown to them by pressing buttons corresponding to A, B, C, and D. Data were collected in a list mode format.

PET data from the latter scan of study I was used in study **III**.

### 4.3.3 Image Preprocessing

In study **I**, the list mode format data was histogrammed using the following sequence of frames:  $2 \times 30$ ,  $9 \times 60$ ,  $3 \times 120$ ,  $3 \times 180$ , and  $6 \times 300$  seconds, resulting in a total of 23 frames. Image estimates with isotropic voxel dimensions of  $1.22 \text{ mm} \times 1.22 \text{ mm} \times 1.22 \text{ mm}$  were generated using a speed-optimized version of ordinary Poisson ordered subsets expectation maximization (OP-OSEM-3D) reconstruction with 16 subsets and 8 iterations. Then dynamic [ $^{11}\text{C}$ ]raclopride images were processed using SPM2 (Wellcome Trust Centre for Neuroimaging, London, UK). First, head positioning between the two PET scans was corrected with PET-to-PET realignment between the sum images. For anatomic reference, T1-weighted magnetic resonance images were co-registered to a mean image of the realigned PET images. Frame-to-frame co-registration considered to be unnecessary based on external motion recordings.

For image reconstruction with fixed counting statistics a new set of sinograms with more constant noise characteristics was generated by fixing the minimum counts at  $7 \times 10^6$  NEC per frame.

$$NEC = \frac{T^2}{T + S + 2R}$$

where T denotes the number of trues, S is the number of scattered, and R the number of random events. NEC-based framing produced 10 to 17 frames per scan, depending on the injected dose and the weight of the subject. Furthermore, parts of each scan were rebinned into frames with extremely low count statistics, yielding  $5 \times 10^5$  to  $2 \times 10^6$  NECs in 268 frames. A resolution model algorithm was also implemented into OP-OSEM-3D as described in earlier papers (Sureau et al. 2008 Comtat et al. 2008). The resolution modeling uses a measured point-spread function (PSF) of the scanner, which is assumed to be space invariant within the field of view. The same iteration number (10), and number of subsets (16) were used as in the earlier publication of Comtat et al. (2008). Areas under the curve (AUC) were calculated from both the original and new sets of time–activity data and changes from original data were calculated as follows:

$$\Delta AUC = \frac{\int_{t_1}^{t_2} f(t) dt - \int_{t_1}^{t_2} f_0(t) dt}{\int_{t_1}^{t_2} f_0(t) dt}$$

where  $f_0$  is the time–activity course estimated with the original framing. Integrals of the discrete time–activity course data were calculated with an in-house software with linear interpolation. It was decided to define  $\Delta AUC(\%) = 100\% \Delta AUC$ . The rebinned sinogram data were reconstructed into image data in the same way as the original data, described above.

In study **II**, PET image reconstructions were devised using the ordinary OP-OSEM algorithm with 16 subsets and 8 iterations and a voxel size of  $1.22 \text{ mm} \times 1.22 \text{ mm} \times 1.22 \text{ mm}$ . The used time–framings were  $8 \times 2$ ,  $4 \times 3$ ,  $2 \times 4$ ,  $1 \times 5$ ,  $1 \times 6$ , and  $1 \times 8$  minutes. Dynamic image data were first corrected for frame-by-frame and between-scan misalignments using the realign function in SPM8. Then anatomic T1 MR images were co-registered to a PET sum image for anatomic reference. MR tissue segmentation and spatial normalization were done using the unified segmentation algorithm in SPM8. Unified segmentation yielded tissue probability maps for gray and white matter and deformation fields for mapping individual images into Montreal Neurological Institute space and, conversely for mapping images in Montreal Neurological Institute space into individual space.

In study **III**, image reconstructions were created using the ordinary OP-OSEM algorithm with resolution modeling and 10 iterations and 16 subsets. Realignments, co-registrations and normalizations were performed in SPM8, revision 4290, with re-slicing into a voxel size of  $1.5 \text{ mm} \times 1.5 \text{ mm} \times 1.5 \text{ mm}$ . First, dynamic image data were corrected for frame-by-frame misalignments with a sum of initial frames as the reference. Co-registration of the MR image was executed to the motion-corrected PET data, again using the sum of initial frames as the reference. Voxel-wise kinetic modeling was done with the basis

function (BF) implementation of SRTM. Voxel-wise modeling generated an image of the  $BP_{ND}$  estimates at each voxel. These voxel-wise maps were then registered into MNI space using a [ $^{11}C$ ]raclopride template and SPM8 normalization routine. The [ $^{11}C$ ]raclopride template was obtained by mapping the T1 MR images onto a T1 MR template and applying the same mapping to the co-registered PET data.

#### 4.3.4 Region of Interest Analysis

In study **I**, regions of interest were drawn using in-house software, Imadeus version 1.2 (Forima, Turku, Finland) on coregistered MR images. Thus, an identical set of ROIs was defined for both [ $^{11}C$ ]raclopride scans of the same subject. The ROIs were applied in the transaxial orientation on the caudate nucleus, putamen, VST, thalamus and cerebellum. The thalamus was divided into its medial and lateral parts. In addition, VST was drawn also in the coronal plane according to Mawlawi et al. (2001).

In study **II**, subcortical ROIs and reference region were drawn using in-house software (Carimas 2.8, Turku PET Centre, Turku, Finland) on co-registered MR images. Thus, an identical set of ROIs was applied for both of the subject's [ $^{11}C$ ]raclopride scans. ROIs were defined in the coronal orientation for the caudate nucleus, putamen, and VST. The caudate nucleus and putamen were divided into pre-commissural and post-commissural sections. The VST was defined according to Mawlawi et al. (2001). The thalamic and cerebellar ROIs were drawn on trans-axial slices. Neocortical ROIs were created using FreeSurfer software (version 5.3; <http://surfer.nmr.mgh.harvard.edu/>), which can be used to produce high anatomical accuracy ROIs for PET data analysis (Dreve et al. 2014). The automatic processing of T1-weighted MR images with FreeSurfer includes removal of nonbrain tissue, segmentation of subcortical structures, automated Talairach transformation, intensity normalization, tessellation of the gray–white matter boundary, automated topology correction, and surface deformation after intensity gradients to optimally define the tissue boundaries at the location where the maximum shift in intensity defines the transition to the other tissue class (more details in <http://surfer.nmr.mgh.harvard.edu/>). The results of the automatic processing were visually reviewed and manually corrected if deemed necessary. Cortical gray matter was enclosed with a probabilistic labeling algorithm by inflating the gray–white matter barrier with the overlaying curvature information of the surface inflated. Neocortical ROIs included anterior cingulate, superior frontal gyrus, inferior frontal gyrus, dorsolateral prefrontal cortex (DLPFC), orbitofrontal cortex (OFC), and temporal cortex.

In study **III**, ROIs were drawn on average MRI slices in coronal orientation using in-house software (Carimas 2.4, Turku PET Centre, Turku, Finland). ROIs included the caudate nucleus, putamen and VST. Cerebellar ROIs were drawn in axial planes. For the caudate nucleus, the region sampled was from the level of -21 mm to the level of 6 mm relative to

the level of anterior commissure (AC=0 mm) and thus contained 19 planes. The putamen was sampled from its anterior border of -16.5 mm to the level of 15 mm, including 22 planes. The VST was defined according to Mawlawi et al. (2001) and was sampled from the level of -12 mm to the level of -6 mm; thus it consisted of 5 planes (See figure 7a and b).

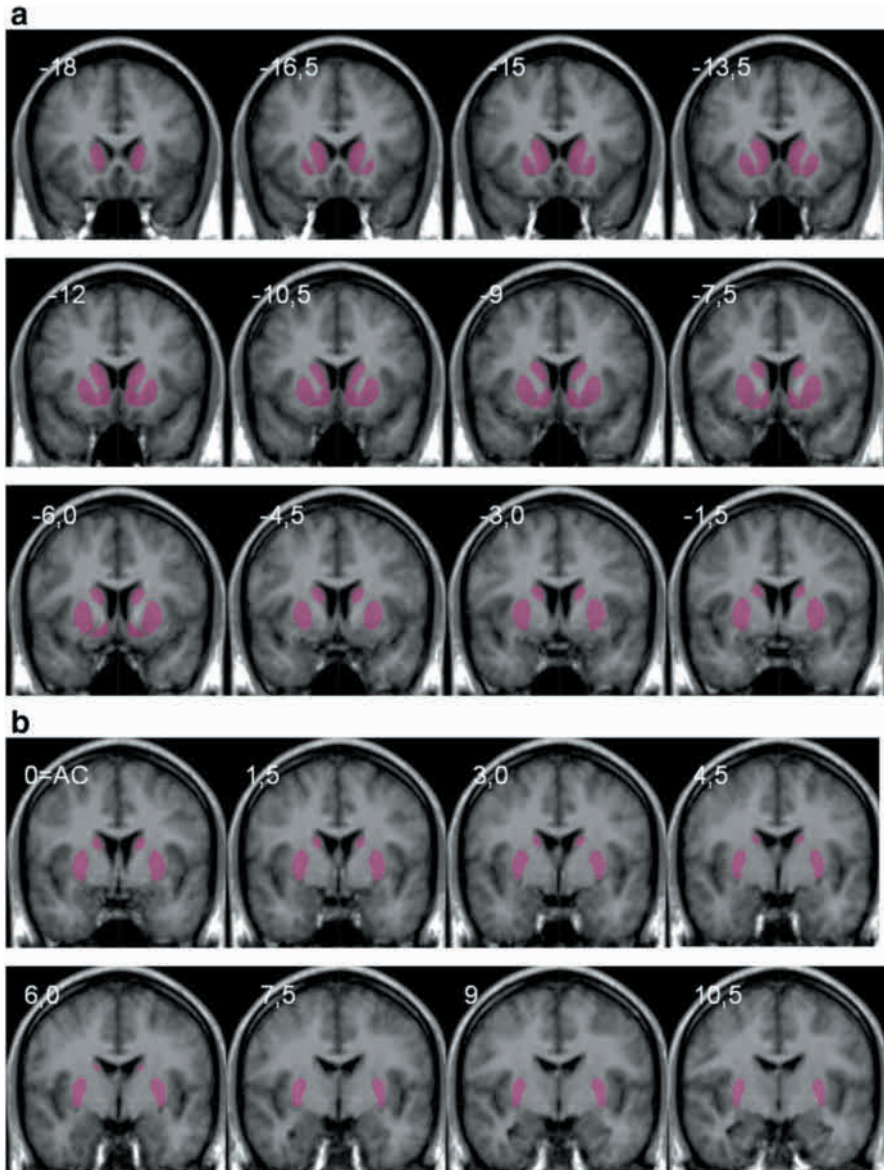


**Figure 7. a)** A sample of coronal MRI slices showing regions of interest (ROIs) of the caudate nucleus, putamen and ventral striatum (VST) rostral to the level of anterior commissure (AC = 0 mm). The anterior slices presented here originate from the level of -18 mm to -1.5 mm. **b)** A sample of coronal MRI slices showing regions of interest (ROIs) of the caudate nucleus, putamen and ventral striatum (VST) caudal to the level of anterior commissure (AC = 0 mm). The posterior slices presented here originate from the level of 0 mm to 10.5 mm. (Alakurtti et al. 2013)

### 4.3.5 Quantification of [<sup>11</sup>C]raclopride Binding

Specific [<sup>11</sup>C]raclopride binding to D2/3R was calculated using the simplified reference tissue compartmental modeling (SRTM) (Lammertsma and Hume 1996) at both ROI and voxel levels. The cerebellum was selected as reference tissue, since it is known to be devoid of D2/3R (Hall et al. 1988). In the ROI-level model fitting, a nonlinear, weighted fitting was applied based on actual count statistics implemented in an in-house software ([http://www.turkupertcentre.net/software/doc/fit\\_srtm\\_3\\_1\\_0.xml](http://www.turkupertcentre.net/software/doc/fit_srtm_3_1_0.xml)). We used a linearized model using a basis-function approach (Gunn et al. 1997) for voxel-level model fitting. This is also implemented in in-house software (<http://www.turkupertcentre.net/programs/doc/imgbfbp.html>). In study **II**, in addition to the STRM based modeling, the ratios of area under the curve during equilibrium condition from 36 to 55 minutes were also used to calculate BP<sub>ND</sub> values. In this method, radioactivity concentration ratios of the target region and cerebellar reference region are calculated using the formula BP<sub>ND</sub>=target-reference/reference (from now on denoted as ratio method (RM)) (Carson et al. 1997). In study **III**, the mean BP<sub>ND</sub> was sampled plane-by-plane, 1.5 mm apart, on spatially normalized parametric images of each substriatal region.

## 4.4 STATISTICAL ANALYSIS

In study **I** and **II** the test–retest variability (VAR%) was calculated as follows:

$$VAR = \frac{2|T - RT|}{T + RT} \times 100\%$$

where the first (test) estimate is denoted as T and RT is the second (retest) estimate. Test–retest reliability was measured using an intra-class correlation coefficient (ICC).

$$\frac{BSMSS - WSMSS}{BSMSS + (n - 1)WSMSS}$$

The ICC can have a value between -1 and 1. Values closer to 1 indicate that most of the variance is due to between-subject rather than within-subject variation, which indicates good reliability. Values below 0 indicate greater within-subject than between-subject variation designating poor reliability. Paired two-tailed *t*-tests were used to detect significant differences between the BP<sub>ND</sub> estimates, injected doses, specific radioactivities, injected masses, of the test and the retest scans. Statistical analyses were performed to BP<sub>ND</sub> estimates at both ROI and voxel levels. In study **III** in order to assess the correlation between the location of the plane and the BP<sub>ND</sub> values, the Pearson correlation coefficient (*r*), the non-parametric Spearman correlation coefficient (*r<sub>s</sub>*) and a second-order regression analysis (*R*) were applied. *P* = 0.05 was chosen as the level of significance.



## 4.5 MOTION DATA

In all (I-III) studies, individual thermoplastic masks were used for each subject to minimize head movements. An external position detector (Polaris Vicra, Northern Digital, Waterloo, Ontario, Canada) was used to monitor head motion. The Polaris Vicra system (Northern Digital) tracks the position of passive infrared reflectors that are placed on top of the mask of the forehead close to the central line. The average position of the reflectors was recorded over the transmission scans, which were used as the reference for later tracking. External-motion estimates were calculated as the position difference between the reference and a given time point. Frame-to-frame motion estimates were obtained using the `realign` function of SPM8 (Wellcome Trust Centre for Neuroimaging), which uses a mutual information maximization algorithm for rigid image registration. In study I, the head motion was within the scanner's resolution (~2.5 mm) and thus motion correction was deemed unnecessary. In study II, the initial 4-6 minutes frame was used as a reference to obtain as low as possible within-frame motion and high-count statistics. Each frame was then co-registered with the reference frame and a transformation matrix was used to generate motion-corrected image sequences, and to calculate the amount of misalignment from the reference point. Frame-to-frame displacement from the reference point within SPM8 was compared with average displacement of the Polaris (Northern Digital) with very good agreement. Thus, frame-to-frame motion estimates from SPM8 were used to exclude suspect data from final analysis. Displacements over 2.0 mm from the reference point were regarded as being critical, and if this threshold was exceeded in more than 10% of all frames in either of the scans, the subject was left out from test-retest analysis. In study III, dynamic image data were corrected for frame-by-frame misalignments with a sum of initial frames as the reference, as described above.

## 5. RESULTS

### 5.1 REPRODUCIBILITY OF STRIATAL AND THALAMIC D2/3R BINDING (I)

The mean  $BP_{ND}$  values ranged from  $0.65 \pm 0.04$  to  $4.41 \pm 0.47$  with the conventional framing using the OP-OSEM-3D reconstruction (Table 1). The  $BP_{ND}$  was highest in the putamen, followed by the caudate nucleus and VST. Thalamic  $BP_{ND}$  values were lowest and were almost identical for the medial and lateral sections ( $0.65 \pm 0.04$  and  $0.67 \pm 0.04$ , respectively). No noticeable lateralization of the [ $^{11}C$ ]raclopride binding was observed ( $P=0.18-0.98$  for test, and  $P=0.08-0.94$  for retest) and also the VAR values were nearly identical in both left and right hemispheres ( $P=0.30-0.93$ ).

The test–retest VAR (%) and ICC values are also presented in Table 1. Mean VAR (%) values were 3.7% and 4.7% for the caudate nucleus and putamen, and 4.6% and 6.7% for the lateral and medial thalamus, indicating fairly good reproducibility in these regions. In the putamen, ICC was high, (0.87). In the caudate nucleus, ICC was only moderate (0.59). Thalamic ICC values were moderate (0.44 for the lateral part and 0.66 for the medial part). For the VST, the ROIs defined in the coronal plane yielded higher  $BP_{ND}$  values than the ROIs drawn in the axial plane ( $3.42 \pm 0.23$  versus  $3.22 \pm 0.32$ , respectively). In addition, the VAR (5.9%) and the ICC (0.50) were superior for the coronally defined VST ROIs as compared with those drawn on the axial plane (9.7% and 0.34, respectively).

**Table 1.** Regional [ $^{11}C$ ]raclopride  $BP_{ND}$  values with original reconstruction and their test–retest characteristics.  $BP_{ND}$ , binding potential according to the simplified reference tissue model; COV, coefficient of variation; ICC, intraclass correlation coefficient;  $M \pm s.d.$ , mean  $\pm$  standard deviation; VAR, absolute variability

REGION	Scan 1		Scan 2		Both scans	VAR (%)	100x (Scan2 -Scan1) /Scan 1	t-test sign.	ICC
	Mean $\pm$ SD	COV (%)	Mean $\pm$ SD	COV (%)					
putamen	4.33 $\pm$ 0.45	10.32	4.49 $\pm$ 0.51	11.36	4.41 $\pm$ 0.47	4.70 $\pm$ 3.91	-2.76 12.08	0.104	0.87
caudate nucleus	3.81 $\pm$ 0.22	5.83	3.88 $\pm$ 0.23	6.05	3.85 $\pm$ 0.22	3.71 $\pm$ 4.72	-4.24 12.37	0.402	0.59
ventral striatum (cor)	3.40 $\pm$ 0.28	8.34	3.44 $\pm$ 0.26	7.51	3.42 $\pm$ 0.26	5.93 $\pm$ 5.34	-8.84 15.37	0.731	0.50
ventral striatum (ax)	3.27 $\pm$ 0.43	13.13	3.17 $\pm$ 0.36	11.41	3.22 $\pm$ 0.38	9.72 $\pm$ 9.67	-20.06 24.96	0.599	0.34
medial thalamus	0.65 $\pm$ 0.03	5.03	0.68 $\pm$ 0.05	7.12	0.67 $\pm$ 0.04	4.59 $\pm$ 3.22	0.49 9.85	0.010	0.66
lateral thalamus	0.63 $\pm$ 0.05	7.27	0.67 $\pm$ 0.04	5.67	0.65 $\pm$ 0.04	6.69 $\pm$ 4.82	-1.77 11.51	0.024	0.44

There was an increase in the mean of  $BP_{ND}$  values from test to retest scans in all regions except in the VST. The increase was statistically significant only in the lateral ( $P=0.02$ ) and medial thalamus ( $P=0.01$ ). There were no statistically significant differences in the injected doses, specific radioactivities or in the injected masses between the test and retest scans. However, one outlier (injected mass of  $13.03 \mu\text{g}$ ) was detected in the boxplot analysis, which is considerably higher than the average of the other values. Theoretically, a low specific activity of [ $^{11}\text{C}$ ]raclopride would lead to an underestimation of the  $BP_{ND}$ . Exclusion of this outlier with low specific radioactivity from the analysis decreased the difference between mean  $BP_{ND}$  in the test and retest scans and produced slightly superior VAR and ICC values (data not shown).

$BP_{ND}$  estimates and the VAR and ICC values using the high statistics framing are presented in Table 2. As compared with the conventional framing, changes in the mean  $BP_{ND}$  were positive in the caudate nucleus (2.86%), in the putamen (2.95%), in the axially drawn VST (2.17%), and in the coronally drawn VST (2.05%), and negative or zero in the lateral (-1.59%) and medial parts of thalamus (0.00%). High counting statistics yielded higher VAR in the caudate nucleus, the putamen, and in the lateral part of thalamus, but lower VAR in the medial part of thalamus and in the VST. None of the regions had significantly different mean VAR when compared with the original framing. The high counting statistics improved the ICC in the thalamus and in VST defined in coronal planes, whereas in other regions, the change was either negative or zero.

**Table 2.** Regional [ $^{11}\text{C}$ ]raclopride  $BP_{ND}$  values with high counting statistics reconstructions and their test–retest characteristics.  $BP_{ND}$ , binding potential according to the simplified reference tissue model; COV, coefficient of variation; ICC, intraclass correlation coefficient;  $M\pm s.d.$ , mean $\pm$ standard deviation; VAR, absolute variability.

REGION	Scan 1		Scan 2		Both scans	VAR (%)	100x (Scan2-Scan1)/Scan1	t-test sign.	ICC
	Mean $\pm$ SD	COV (%)	Mean $\pm$ SD	COV (%)					
putamen	4.46 $\pm 0.49$	10.89	4.62 $\pm 0.54$	11.72	4.54 $\pm 0.50$	5.03 $\pm 3.84$	-2.93 12.27	0.138	0.87
caudate nucleus	3.92 $\pm 0.24$	6.16	3.99 $\pm 0.23$	5.88	3.96 $\pm 0.23$	4.00 $\pm 4.70$	-3.95 12.37	0.430	0.57
ventral striatum (cor)	3.47 $\pm 0.27$	7.84	3.52 $\pm 0.28$	7.86	3.49 $\pm 0.26$	5.65 $\pm 5.73$	-7.34 16.22	0.674	0.51
ventral striatum (ax)	3.34 $\pm 0.42$	12.45	3.25 $\pm 0.37$	11.51	3.29 $\pm 0.38$	9.53 $\pm 9.90$	-19.37 25.45	0.639	0.31
medial thalamus	0.65 $\pm 0.04$	6.82	0.68 $\pm 0.06$	8.59	0.67 $\pm 0.05$	4.51 $\pm 3.10$	1.94 9.32	0.011	0.78
lateral thalamus	0.62 $\pm 0.05$	7.85	0.65 $\pm 0.04$	5.69	0.64 $\pm 0.04$	6.81 $\pm 3.63$	-3.82 12.04	0.077	0.51

The  $BP_{ND}$  estimates, the mean VAR, and the ICC values using PSF reconstruction are presented in Table 3. The PSF reconstruction produced higher  $BP_{ND}$  estimates in all regions except in the lateral thalamus when compared with the original framing using the non-PSF reconstruction. The increases were most evident in the caudate nucleus and putamen. However, VAR values were increased and ICC values decreased in many of the regions. The largest increase in VAR was observed in the caudate nucleus and putamen, whereas the VAR was somewhat smaller in the VST. The ICC values were decreased in all regions except the lateral thalamus.

**Table 3.** Regional [ $^{11}C$ ]raclopride  $BP_{ND}$  values with PSF reconstructions and their test–retest characteristics.  $BP_{ND}$ , binding potential according to the simplified reference tissue model; COV, coefficient of variation; ICC, intraclass correlation coefficient;  $M\pm s.d.$ , mean $\pm$ standard deviation; VAR, absolute variability

REGION	Scan 1		Scan 2		Both scans	VAR (%)	100x (Scan2-Scan1)/Scan1	t-test sign.	ICC
	Mean	COV (%)	Mean	COV (%)	Mean	Mean	RANGE		
	$\pm SD$		$\pm SD$		$\pm SD$	$\pm SD$			
putamen	4.75 $\pm 0.49$	10.41	4.93 $\pm 0.57$	11.67	4.84 $\pm 0.52$	5.76 $\pm 4.32$	-3.90 14.08	0.158	0.82
caudate nucleus	4.21 $\pm 0.24$	5.65	4.29 $\pm 0.25$	5.92	4.25 $\pm 0.24$	4.78 $\pm 5.44$	-4.68 15.26	0.497	0.35
ventral striatum (cor)	3.65 $\pm 0.27$	7.48	3.71 $\pm 0.27$	7.37	3.68 $\pm 0.26$	5.56 $\pm 5.57$	-6.83 14.77	0.601	0.48
ventral striatum (ax)	3.57 $\pm 0.45$	12.7	3.46 $\pm 0.38$	10.96	3.52 $\pm 0.41$	9.17 $\pm 9.60$	-20.18 23.31	0.587	0.33
medial thalamus	0.66 $\pm 0.04$	6.28	0.70 $\pm 0.06$	8.92	0.68 $\pm 0.06$	6.07 $\pm 3.88$	0.71 10.29	0.007	0.64
lateral thalamus	0.59 $\pm 0.06$	9.55	0.63 $\pm 0.05$	7.54	0.61 $\pm 0.05$	9.09 $\pm 3.37$	-5.09 13.77	0.021	0.52

## 5.2 LONG TERM TEST RETEST RELIABILITY OF STRIATAL AND EXTRASTRIATAL DOPAMINE D2/3R BINDING (II)

Regional [ $^{11}C$ ]raclopride  $BP_{ND}$  values and their test–retest characteristics are shown in Table 4.  $BP_{ND}$  values are expressed as the mean $\pm$ s.d. In the striatum,  $BP_{ND}$  values were high in all subregions, in the range of  $3.48\pm 0.27$  to  $4.55\pm 0.37$ . Thalamic  $BP_{ND}$  was  $0.70\pm 0.06$  and cortical  $BP_{ND}$  values ranged from  $0.30\pm 0.06$  to  $0.38\pm 0.07$ . There were no significant differences in [ $^{11}C$ ]raclopride binding between scans in any of the regions measured ( $P=0.17-0.97$ ). No noticeable lateralization was detected in the striatal regions ( $P=0.17-0.98$  for test and  $P=0.44-0.94$  for retest). In the cortex, there was lower  $BP_{ND}$  in the left superior frontal gyrus and caudal frontal middle cortex (data not shown).

**Table 4.** Regional [<sup>11</sup>C]raclopride BP<sub>ND</sub> values and their test-retest characteristics. \_A = anterior; BP<sub>ND</sub> = binding potential according to the simplified reference tissue model (SRTM); CING\_A = Anterior cingulate; COV = coefficient of variation; DLPFC = dorsolateral prefrontal cortex; ICC = intraclass correlation coefficient; M±s.d. = mean±standard deviation; OFC = orbitofrontal cortex; \_P = posterior; VAR = absolute variability.

Region	Scan 1 (BPND)			Scan 2 (BPND)			Both Scans (BPND)			Between Scans			
	Mean ±SD	COV (%)	Mean ±SD	Mean ±SD	COV (%)	Mean ±SD	Mean ±SD	COV (%)	Mean ±SD	Mean ±SD	Range	Diff. (%)	t-test
Putamen	4.47 ±0.40	8.86	4.41 ±0.29	6.58	4.44 ±0.34	3.93 ±2.41	7.55	4.72	3.93 ±2.41	7.55	-6.71 4.72	0.44	0.83
Putamen_A	4.32 ±0.36	8.31	4.30 ±0.26	6.05	4.31 ±0.30	4.34 ±3.36	6.99	6.72	4.34 ±3.36	6.99	-8.19 6.72	0.84	0.72
Putamen_P	4.60 ±0.42	9.21	4.50 ±0.33	7.32	4.55 ±0.37	3.53 ±2.16	8.09	2.96	3.53 ±2.16	8.09	-5.67 2.96	0.19	0.88
Caudate nucleus	4.07 ±0.38	9.30	4.07 ±0.29	7.10	4.07 ±0.32	4.52 ±2.64	7.95	7.7	4.52 ±2.64	7.95	-6.39 7.7	0.97	0.82
Caudate nucleus_A	4.10 ±0.39	9.48	4.10 ±0.30	7.29	4.10 ±0.33	4.15 ±3.11	8.12	7.71	4.15 ±3.11	8.12	-6.61 7.71	1.00	0.84
Caudate nucleus_P	3.70 ±0.53	14.22	3.59 ±0.39	11.00	3.64 ±0.45	9.48 ±7.11	12.38	10.94	9.48 ±7.11	12.38	-22.14 10.94	0.53	0.54
Ventral striatum	3.52 ±0.28	7.87	3.45 ±0.29	8.29	3.48 ±0.27	3.92 ±3.26	7.84	6.57	3.92 ±3.26	7.84	-9.58 6.57	0.29	0.82
Thalamus	0.69 ±0.07	9.81	0.70 ±0.06	8.96	0.70 ±0.06	3.67 ±1.25	9.03	5.47	3.67 ±1.25	9.03	-4.25 5.47	0.59	0.92
DLPFC	0.38 ±0.07	19.82	0.38 ±0.07	18.74	0.38 ±0.07	8.76 ±4.87	18.54	16.97	8.76 ±4.87	18.54	-12.62 16.97	0.76	0.86
Anterior cingulate	0.36 ±0.06	15.12	0.37 ±0.06	16.84	0.37 ±0.06	7.36 ±7.91	15.46	19.4	7.36 ±7.91	15.46	-16.37 19.4	0.48	0.84
Inferior frontal gyrus	0.32 ±0.04	13.79	0.35 ±0.05	12.92	0.34 ±0.05	9.68 ±7.75	13.46	20.12	9.68 ±7.75	13.46	-4.3 20.12	0.07	0.64
Superior frontal gyrus	0.30 ±0.05	17.91	0.31 ±0.06	20.94	0.30 ±0.06	13.06 ±7.39	18.77	0.78	13.06 ±7.39	18.77	-15.46 30.25	0.78	0.67
OFC	0.31 ±0.04	13.49	0.33 ±0.05	15.62	0.32 ±0.05	7.48 ±4.25	14.22	13.23	7.48 ±4.25	14.22	-12.53 13.23	0.21	0.86
Temporal cortex	0.32 ±0.03	9.23	0.34 ±0.04	10.80	0.33 ±0.03	6.09 ±3.13	10.01	10.65	6.09 ±3.13	10.01	-4.81 10.65	0.05	0.79

The test-retest variability (VAR%) and ICC values revealed very good reproducibility throughout the striatum (3.5%, 0.88 - 9.5%, 0.54). VAR and ICC in the thalamus were also very good, 3.7% and 0.92, respectively. Cortical areas exhibited good-to-moderate reproducibility, with values of VAR and ICC ranging from 6.1%, 0.79 (temporal cortex) to 13.1%, 0.67 (superior frontal gyrus) respectively. Maps of voxel-level VAR and ICC are presented in Figure 8 A and B. Regional [ $^{11}\text{C}$ ]raclopride  $\text{BP}_{\text{ND}}$  values calculated using RM and their test-retest characteristics are shown in Table 5. There were no statistically significant ( $P=0.28-0.98$ ) differences between the VAR values generated using SRTM and RM in any of the studied regions.

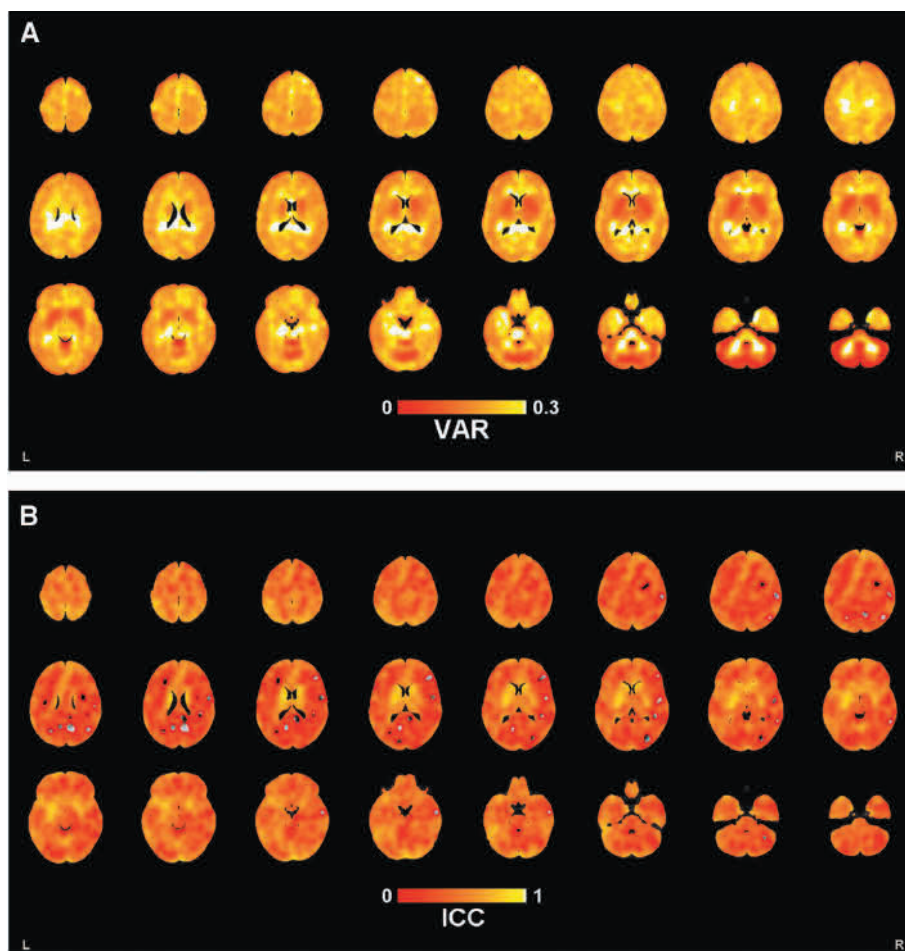


**Figure 8.** (A) Map of voxel-level VAR (absolute variability %) where the (red to yellow) color scale denotes variability from 0% to 30%. Values closer to 0% (red) indicate small variability and closer to 30% (yellow) reflect greater variability between test and retest scans. (B) Map of voxel-level ICC (intra-class correlation coefficient) where the (red to yellow) colorscale represents ICC values between 0 and 1. Values closer to 1 (yellow) indicate that most of the variance is because of between-subject rather than within-subject variation, which is interpreted as good reliability. Negative values indicate the opposite situation (not shown)(Alakurtti et al. 2015).

**Table 5.** Regional [<sup>11</sup>C]raclopride BP<sub>ND</sub> values and their test–retest characteristics. \_A = anterior; BP<sub>ND</sub>, binding potential according to the ratiomethod (RM). CING\_A = Anterior cingulate; COV = coefficient of variation; DLPFC = dorsolateral prefrontal cortex; ICC = intraclass correlation coefficient; M±s.d.= mean±standard deviation; OFC = orbitofrontal cortex; \_P = posterior; VAR = absolute variability.

Region	Scan 1 (BPND)			Scan 2 (BPND)			Both Scans (BPND)			Diff.(%)			Between Scans	
	Mean ±SD	COV (%)	Mean ±SD	COV (%)	Mean ±SD	COV (%)	Mean ±SD	COV (%)	Mean ±SD	Mean ±SD	Range	ICC	t-test	ICC
Putamen	4.36 ±0.42	9.64	4.22 ±0.28	6.59	4.29 ±0.35	8.185,06 ±4.82	-11.9 3.47					0.22		0.65
Putamen_A	4.24 ±0.38	9.05	4.13 ±0.25	5.98	4.18 ±0.32	7.545,2 ±5.28	-12 4.91					0.38		0.54
Putamen_P	4.47 ±0.45	10.02	4.30 ±0.31	7.23	4.39 ±0.38	8.694,84 ±4.48	-11.64 1.95					0.12		0.72
Caudate nucleus	3.99 ±0.40	10.03	3.90 ±0.26	6.78	3.95 ±0.33	8.333,94 ±3.37	-8.34 4.58					0.30		0.82
Caudate nucleus_A	4.01 ±0.41	10.12	3.93 ±0.28	7.08	3.97 ±0.34	8.493,84 ±3.13	-7.84 4.58					0.30		0.84
Caudate nucleus_P	3.62 ±0.58	15.91	3.45 ±0.40	11.49	3.54 ±0.48	13.687,3 ±7.61	-20.61 4.22					0.27		0.70
Ventral striatum	3.43 ±0.27	7.92	3.31 ±0.26	7.76	3.37 ±0.26	7.774,88 ±2.52	-9.24 4.51					0.06		0.78
Thalamus	0.69 ±0.07	9.83	0.70 ±0.07	9.59	0.70 ±0.06	9.348,11 ±6.7	-9.12 24.15					0.81		0.37
DLPFC	0.39 ±0.08	19.88	0.38 ±0.07	18.32	0.38 ±0.07	18.3710,60 ±7.02	-14.03 26.4					0.97		0.75
Anterior cingulate	0.38 ±0.05	11.97	0.37 ±0.07	18.36	0.37 ±0.06	14.898,69 ±8.16	-20.05 7.36					0.46		0.76
Inferior frontal gyrus	0.34 ±0.05	14.39	0.35 ±0.04	10.13	0.35 ±0.04	11.969,03 ±4.59	-11.37 15.52					0.62		0.66
Superior frontal gyrus	0.31 ±0.05	17.62	0.30 ±0.06	20.94	0.31 ±0.06	18.5913,32 ±12.05	-15.8 44.02					0.98		0.50
OFC	0.33 ±0.05	14.55	0.33 ±0.05	15.91	0.33 ±0.05	14.655,92 ±7.05	-18.2 8.83					0.98		0.88
Temporal cortex	0.33 ±0.03	10.36	0.34 ±0.03	9.63	0.34 ±0.03	9.655,28 ±3.22	-5.69 12.45					0.43		0.83

### 5.3 ROSTROCAUDAL GRADIENTS OF DOPAMINE D2/3R BINDING (III)

The  $BP_{ND}$  values along the anterior-posterior (AP) axis of the caudate nucleus, putamen and VST are presented as scatter plots in Figures 9 a, b and c, respectively. Figure 10 shows a three-dimensional maximum intensity projection (MIP) presentation of the normalized average map of  $BP_{ND}$ . The rank order of the mean  $BP_{ND}$  values was putamen > caudate nucleus > VST and ranged from  $2.84 \pm 0.20$  to  $5.10 \pm 0.41$ . Putamen had a significant increasing gradient of mean  $BP_{ND}$ ,  $r = 0.90$ ,  $P < 0.0001$ ;  $r_s = 0.91$ ,  $P < 0.0001$ ;  $R = 0.95$ ,  $P = 0.001$ . A more subtle but still statistically significant descending gradient,  $r = -0.75$ ,  $P = 0.0002$ ;  $r_s = -0.68$ ,  $P < 0.001$ ;  $R = 0.85$ ,  $P = 0.01$  was found in the caudate nucleus. However, in the caudate nucleus, the observed gradient was not necessarily linear because there was an initial increase of the  $BP_{ND}$  values in the first four planes, suggesting that the head of the caudate nucleus had the highest D2/3R binding. A significant declining gradient was found in the VST,  $r = -0.98$ ,  $P = 0.002$ ;  $r_s = -1.0$ ,  $P < 0.0001$ ; however, after second-order regression analysis, the observed gradient did not reach the level of statistical significance ( $R = 0.99$ ,  $P = 0.2$ ).

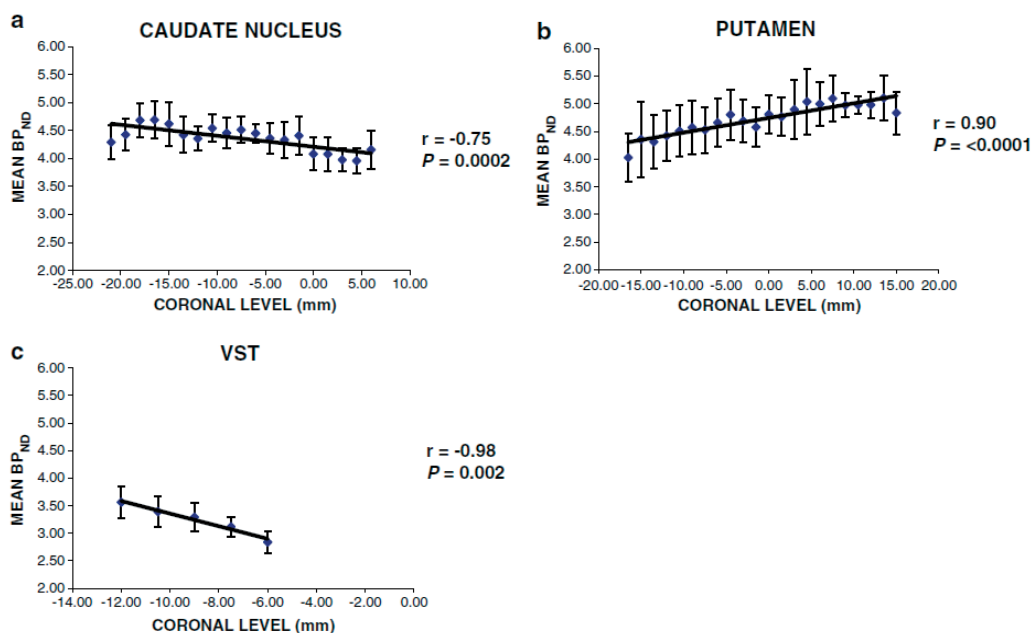


**Figure 9.** Scatter plots of the mean binding potential ( $BP_{ND}$ ) values in each coronal plane of the a) caudate nucleus, b) putamen and c) ventral striatum (VST). X-axis = coronal level (mm, AC = 0 mm), Y-axis = mean  $BP_{ND}$ ,  $r$  = Pearson correlation coefficient,  $P$  = two-tailed t-test, level of statistical significance 0.05 (Alakurtti et al. 2013).



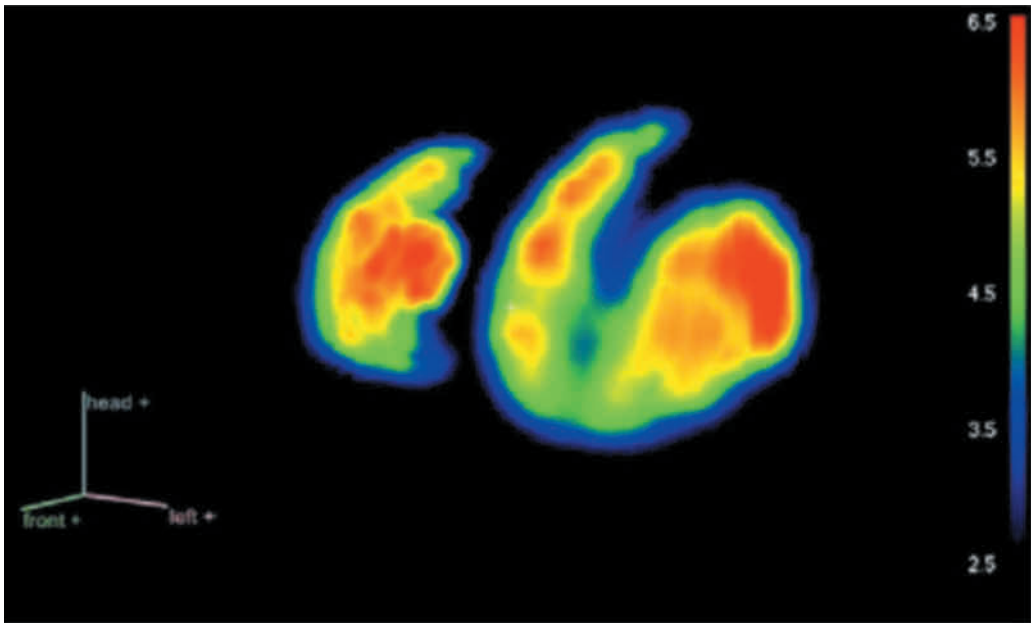


**Figure 10.** A three-dimensional maximum intensity projection (MIP) presentation of the normalized average map of binding potential ( $BP_{ND}$ ) values, where the rostrocaudal gradient is well visualized. Red represents high  $BP_{ND}$ , whereas blue denotes low  $BP_{ND}$  (Alakurtti et al. 2013).

## 6. DISCUSSION

### 6.1 METHODOLOGICAL CONSIDERATIONS

As far as is known, this is the first time test-rest that the reliability of striatal and thalamic dopamine D2/3R binding has been measured using [ $^{11}\text{C}$ ]raclopride and a high-resolution PET scanner, the HRRT scanner (study I). The reproducibility of cortical binding has also been evaluated for the first time per se (study II). Moreover, this is the first time that the rostrocaudal gradients of striatal dopamine D2/3R binding have been evaluated in the living healthy human brain (study III). The HRRT scanner at our disposal meant that it was possible to examine substriatal dopamine D2/3R transmission with the kind of anatomical accuracy not achievable before with the previous generation of whole body PET scanners. This was interesting not only from the methodological point of view but it also made it possible to determine whether many aspects of the normal dopamine neurotransmission and the functional organization of the human striatum could be further verified.

It was known that [ $^{11}\text{C}$ ]raclopride had been one of the most extensively studied PET tracers and its test-retest reliability had been claimed to be excellent. However, the measurement of small substriatal structures such as the VST has been hampered by the partial volume effect caused by the inadequate resolution of the conventional scanners. Furthermore, the long term reproducibility had never been fully established. The long term reproducibility is important when the same subject is studied twice, first at baseline and after a more time consuming pharmacological or non-pharmacological intervention, or in cases where the scans cannot be performed within the same day (e.g. long-lasting effect of the pharmacological intervention).

The term “binding potential” was initially based on *in vitro* radioligand binding and is defined as the ratio of  $B_{\text{max}}$  (receptor density) to  $K_{\text{D}}$  (radioligand equilibrium dissociation constant) (Mintun et al. 1984). The  $\text{BP}_{\text{ND}}$  reflects but does not correlate with the product of  $B_{\text{max}}$  and  $1/K_{\text{D}}$ .  $\text{BP}_{\text{ND}} = f_{\text{ND}} B_{\text{Avail}} (1/K_{\text{D}})$ , where  $B_{\text{Avail}}$  is the density of receptors available for radioligand binding,  $1/K_{\text{D}}$  is the apparent affinity, and  $f_{\text{ND}}$  is the fraction of the radiotracer free within tissue (Innis et al. 2007). *In vitro* assays usually employ homogenized tissue in which all receptors are available for radioligand binding. In contrast, in *in vivo* experiments, only a small fraction of these receptors ( $B_{\text{Avail}}$ ) may be available for radioligand binding since some of these receptors may be in a non-active low affinity state or occupied by an endogenous transmitter. The gradients observed *in vivo* in study III may be attributable to a combination of gradients in high receptor densities and differences in the baseline dopamine occupancy of receptors in living brain tissue. Moreover, estimates of the specific

binding of [ $^{11}\text{C}$ ]raclopride to the D2/3R were measured only over the striatal coronal sections. The selection of orientation was based on the known functional organization of the striatum and on the previous post-mortem studies. Because of the inherently noisy PET data, and the small sample size, the assumption was made that it would have been impossible to obtain statistical significance in a voxel-wise analysis, which obviously rules out the possibility to measure the gradient in a vector field. Thus, ROI-based analysis was chosen for its feasibility and good reproducibility despite the fact that it does not reflect a gradient expressed in a vector field.

Numerous studies have indicated that from early-to-late adulthood, striatal DA function decreases on average by 6%–10% per decade and that there are also regional differences in age-related changes in D2/3R binding (Seeman et al. 1987; Rinne et al. 1993; Antonini et al. 1993; Volkow et al. 1998; Kim et al. 2011). Thus, aging may differentially affect dopamine receptors in various parts of the striatum, resulting in age-related changes in D2/3R gradients in different subregions of the striatum. The subjects examined in study **III** were young healthy males. Thus, the results are not exhaustive considering the whole spectrum of human population. Also, studied sample sizes were relatively small. Future studies using high spatial resolution techniques, multiple radioligands, wider age range, both genders and larger study samples would be highly beneficial.

## 6.2 HRRT PET AND EXPERIMENTAL SIGNAL PROCESSING (I)

This is the first study measuring the reproducibility of [ $^{11}\text{C}$ ]raclopride binding using the HRRT. Noticeably higher [ $^{11}\text{C}$ ]raclopride  $\text{BP}_{\text{ND}}$  values were found in comparison with previous studies using more conventional scanners. For example, 20 % higher  $\text{BP}_{\text{ND}}$  values were measured for the caudate nucleus, putamen, and thalamus than previously reported using a lower-resolution scanner (Hirvonen et al, 2003). In other published reports, a significant increase (30%) in striatal BP values with HRRT has been noted when dopamine transporter (DAT) binding was measured using [ $^{11}\text{C}$ ]-PE2I when these were compared to values obtained with a conventional whole-body PET scanner (Leroy et al, 2007). As the line-of-response (LOR) of the HRRT is significantly thinner than that in the conventional scanners, the counting statistics rather than the spatial resolution become a limiting factor in the quantitative HRRT studies. Thus, the HRRT scanner is associated with a lower signal-to-noise ratio due to a reconstruction bias caused by low count statistics, especially in late frames, and this phenomenon may impair the reliability of the measurement (Johansson et al. 2007; Sureau et al. 2008). This present study implemented a novel approach in PET data sampling and collected a fixed number of counts in each frame, which was made possible by the list mode event recording. The noise-equivalent count (NEC) was applied because it takes into account the varying random rates and scatter fractions. An NEC threshold per frame was extrapolated from a previous

phantom study which evaluated the quantification bias in low statistics (Johansson et al. 2007). NEC-based framing was intended to remove this bias if it was present in this study. The  $BP_{ND}$  values were higher but there was no improvement in either the ICC or the VAR values. Parts of the data were reconstructed with the low count statistics and the bias was estimated directly from the TAC data. A statistically significant decrease in the image contrast was seen when compared with the original framing. The  $BP_{ND}$  estimates were not calculated for low count statistics because there were only a few samples from the beginning and end of each scan. These observations are evidence that the current statistical reconstruction suffers from bias, and this might be of significant magnitude to lead to problems, for instance in follow-up studies if the injected doses vary substantially between scans. Thus, if the injected doses are not sufficiently equivalent, the NEC-based framing could be used to maintain similar conditions for the statistical reconstruction. Ultimately, new bias-free reconstruction schemes must be devised to remove the count statistics limitation in the HRRT studies.

The detector design of the HRRT aims at removing the bias caused by PVE from the PET measurement. Conventionally, the PVE is corrected from the collected data with the help of a variety of algorithms. An implementation of a scanner-specific PSF-based method was recently made for the HRRT users (Comtat et al. 2008). The PSF-based method is reported to be able to generate higher BP estimates as compared with the conventional reconstruction (Sureau et al. 2008; Comtat et al. 2008; Varrone et al. 2009; Mourik et al. 2010). Approximately, 25% higher  $BP_{ND}$  estimates in the caudate nucleus, 23% in putamen, and 10% in VST using  $[^{11}C]$ -PE2I with PSF method have been reported (Sureau et al. 2008). In a study including one human subject imaged with  $[^{11}C]$ -raclopride, ~10% higher  $BP_{ND}$  estimates in the caudate nucleus and 6% higher in the putamen were measured (Varrone et al. 2009). In contrast, in five subjects, no noticeably higher distribution volume estimates with PSF were obtained as compared with non-PSF reconstruction (Mourik et al. 2010). Thus it seems that the improvement with PSF reconstruction is tracer dependent. In this study, ~10% increase was obtained in the  $BP_{ND}$  estimates in the caudate nucleus and putamen and an 8% increase in the VST, which is in line with an earlier report (Varrone et al. 2009). The main objective of the present study was to evaluate the methods with a focus on the reliability of the measurement. Although PSF reconstruction determined  $BP_{ND}$  estimates should be less contaminated by the PVE, the VAR and ICC values were somewhat inferior to the original non-PSF reconstruction. In the thalamus and VST, the VAR and ICC values were identical with the PSF and the non-PSF reconstructions.

It is concluded that the statistical reconstruction of the HRRT is vulnerable to bias attributable to low count statistics, and furthermore the PSF reconstruction increases rather than decreases the VAR values. The PSF reconstruction has been found to be less vulnerable to the low count statistics bias (Planeta-Wilson et al. 2008; Walker et al. 2009).

Here, the PSF reconstruction was not evaluated with regard to count statistics, but it was observed that by using both the fixed high count statistics and the inclusion of the PSF model in the reconstruction it was possible to enhance the contrast of the images. A fixed number of counts did not improve the reproducibility or the reliability of the measurement.

### 6.3 TEST-RETEST RELIABILITY OF STRIATAL AND THALAMIC MEASUREMENTS (I, II)

In study **I**, using conventional framing, the VAR values were 3.7% in the caudate nucleus and 4.7% in the putamen. VAR was 5.9% in the VST when defined in the coronal plane and 9.7% when drawn in the axial plane. Thus, reproducibility was better when using coronal ROIs of the VST, most likely due to the more accurate anatomic delineation with the coronal view. The reproducibility of striatal [<sup>11</sup>C]raclopride binding has been explored earlier in various studies (Volkow et al, 1993; Hietala et al, 1999; Mawlawi et al, 2001; Hirvonen et al, 2003), but not with a high-resolution tomography. The last study in which striatal and thalamic D2/3R binding was quantified, reported VAR values of 5.3% for the caudate nucleus, 3.5% for the putamen, and 8.6% for the VST (Mawlawi et al, 2001). In study **I**, thalamic VAR and ICC values were 4.6%, 0.66 (medial part) and 6.7%, 0.44 (lateral part) and in study **II**, 3.7%, 0.92, respectively. Thalamic results are clearly superior to the results obtained by Mawlawi et al. (2001) (17.4%, 0.39). This is probably due to the higher signal enabled by the superior resolution of the HRRT and also due to the protocol optimization in study **II**. However, the ICC values in study **I** were slightly lower than previously reported for every region except for the putamen. In paper **I**, it was speculated that this discrepancy might at least partly be explained by the small between-subject variability in the study group which resulted in low COV (%) (coefficient of variation) that refers to the extent of variability in relation to the mean of the population values. It was also hypothesized that methodological differences, such as the B/I method used by Mawlawi et al. (2001) could be one explanation for the differences in ICC values. However, in study **II**, the COV (%) was again lower than in previous studies performed with lower resolution techniques, while ICC values were high. Moreover, B/I method was used method in study **II**. Thus, the low ICC values in study **I** cannot be fully explained by either small between-subject variability or by differences in methodological aspects. The most likely explanation for the discrepancy in ICC values might be the fact that one outlier (injected mass of 13.03  $\mu$ g) was detected in the boxplot analysis, which is considerably higher than the average of others. Theoretically, the low specific activity of [<sup>11</sup>C]raclopride would lead to an underestimation of the BP<sub>ND</sub>. The exclusion of this outlier with low specific radioactivity from the analysis decreased the difference between mean BP<sub>ND</sub> in the test and retest scans and produced slightly superior VAR and ICC values (data not shown).

Most previous experiments have examined short-term test-retest reliability with scans taken within 24 hours. There is one previous study on long-term reproducibility of [<sup>11</sup>C]raclopride binding, where two sets of scan pairs (intervals of 3 to 7 weeks and 6 to 11 months) were used (Hietala et al. 1999). These authors reported striatal VAR of 5.5% with a 3-7 week interval, but when the interval was increased to 6 to 11 months, VAR rose to 10.4%. In study II, the scan interval was prolonged to 5 weeks and the VAR and ICC obtained for the whole striatum were excellent: 3.9% and 0.86, respectively. Substriatal results were also very good, ranging from 3.5%, 0.88 (posterior putamen) to 9.5%, 0.54 (posterior caudate nucleus). It should be noted that the volume of the post-commissural caudate is rather small, causing an increased partial volume effect (PVE) and noise, both of which impact negatively on reproducibility. In addition to SRTM based modeling, the RM based modeling was used in study II, because RM is considered to be a gold standard in activation-type studies when using a B/I protocol (Carson et al. 1997). The validity of both SRTM and RM modeling using B/I of [<sup>11</sup>C]raclopride has previously been assessed by Mawlawi et al. (2001), and they found SRTM and RM (denoted in their paper as “equilibrium V3”) to yield very similar results. In their test-retest analyses, SRTM provided slightly better reproducibility in the caudate nucleus and putamen and equivalent reproducibility in the VST and thalamus. In the present study, SRTM and RM based BP<sub>ND</sub> showed rather equivalent reproducibility for [<sup>11</sup>C]raclopride binding and no statistically significant differences in VAR values were detected in any regions measured ( $P = 0.28-0.98$ ). Altogether, these present results are in good agreement with previous test-retest reports and indicate very good short- and long-term reliability of [<sup>11</sup>C]raclopride binding in human striatum, further validating the use of [<sup>11</sup>C]raclopride in imaging D2/3R functions.

## 6.4 TEST-RETEST RELIABILITY OF CORTICAL MEASUREMENTS (II)

VAR and ICC values of cortical [<sup>11</sup>C]raclopride binding ranged from 6.1%, 0.79 (temporal cortex) to 13.1%, 0.67 (superior frontal gyrus), respectively. Stokes et al. (2010) estimated reproducibility of cortical [<sup>11</sup>C]raclopride binding from a separate cohort of control subjects in a study where  $\Delta^9$ -tetrahydrocannabinol (THC) was administered in order to quantify possible alterations of DA transmission in the human cortex. ROI analyses including areas such as right middle frontal gyrus, left superior frontal gyrus and left superior temporal gyrus produced relatively poor VAR values ranging from 18% to 24%. Studies using high-affinity ligands such as [<sup>18</sup>F]fallypride and [<sup>11</sup>C]FLB 457 have reported cortical test-retest reliability of ~10% and 5.3% - 10.4%, respectively (Vilkman et al. 2000; Mukherjee et al. 2002). Thereby, the results of the present study are clearly superior to the previous results of Stokes et al. (2010) and comparable to the test-retest parameters obtained with high-affinity ligands (Vilkman et al. 2000; Mukherjee et al. 2002).

The density of D2/3R in extrastriatal regions is approximately only 2%–8% of that in the striatum (Suhara et al. 1999). [ $^{11}\text{C}$ ]raclopride has moderate *in vivo* affinity and a relatively low signal-to-noise ratio (affinity compared to nonspecific binding) in low D2/3R density areas such as the cortex. Thus, [ $^{11}\text{C}$ ]raclopride is considered as being non-ideal for quantifying D2/3R availability in those areas (Farde et al. 1988). The high-affinity radioligands such as [ $^{11}\text{C}$ ]FLB 457 and [ $^{18}\text{F}$ ]fallypride have been recommended for quantifying extrastriatal D2/3R (Halldin et al. 1995; Olsson et al. 2004). However, these ligands are not optimal in all cases. [ $^{11}\text{C}$ ]FLB 457 is cleared from the striatum much more slowly than [ $^{11}\text{C}$ ]raclopride so that washout of the ligand from the striatum becomes too slow to allow quantitative imaging when coupled with the rapid decay rate of C-11 (Laruelle et al. 2003). Thus, [ $^{11}\text{C}$ ]FLB 457 can only be used in quantifying extrastriatal regions. With [ $^{18}\text{F}$ ]fallypride, it is possible to provide simultaneous measures of D2/3R binding in the striatum and in extrastriatal regions by prolonging the scanning time, but it is impossible to perform two scans within the same day due to the long decay of  $^{18}\text{F}$ . This fact may impair the reliability of the measurement and decrease the possibilities to detect subtle changes in  $\text{BP}_{\text{ND}}$ .

Although [ $^{11}\text{C}$ ]raclopride is not fully optimal for measuring extrastriatal DA transmission, decreases in [ $^{11}\text{C}$ ]raclopride  $\text{BP}_{\text{ND}}$  have been observed in extrastriatal regions following drug or behavioral challenges (Piccini et al. 2003; Sawamoto et al. 2008; Stokes et al. 2010). Brain pathology, such as encountered in Parkinson's, Huntington's, and Alzheimer's diseases, has been demonstrated to cause changes in extrastriatal [ $^{11}\text{C}$ ]raclopride binding (Joyce et al. 1998; Ribeiro et al. 2009; Politis et al. 2011). Thus, as major neurodegenerative disorders have been associated with alterations in cortico-striatal circuits, it would be a major advantage to conduct simultaneous imaging of striatal and extrastriatal regions. There was an acceptable test-retest reliability of [ $^{11}\text{C}$ ]raclopride binding to extrastriatal D2/3R observed in this study; this is in contrast to previous attempts to convincingly demonstrate extrastriatal [ $^{11}\text{C}$ ]raclopride binding. In the early study of Farde et al. (1988), it was demonstrated that in the temporal and frontal cortices, the [ $^{11}\text{C}$ ]raclopride distribution ratios were only a few per cent higher than for the inactive enantiomer of raclopride, [ $^{11}\text{C}$ ]FLB 472, which they interpreted to mean that if D2/3R were present in the human neocortex, their density was too low to be detected. However, one has to remember that during the last almost 30 years or research, the sensitivity and resolution of the PET scanners have improved considerably, not to mention improvements in other methodological aspects. Also the protocol optimization by eliminating the effect of movement and homogenizing the scanning conditions (simple cognitive task) may have contributed to this positive outcome. However, based on the present results, it is not possible to conclude definitively that [ $^{11}\text{C}$ ]raclopride is able to reflect the *specific binding* to D2/3R in the cortical areas. Further work e.g. displacement studies using haloperidol, is needed in confirming whether [ $^{11}\text{C}$ ]raclopride can be used to explore D2/3R in extrastriatal areas.

## 6.5 ROSTROCAUDAL GRADIENTS OF D2/D3R BINDING (III)

There was a significant increasing gradient of [ $^{11}\text{C}$ ]raclopride  $\text{BP}_{\text{ND}}$  values in the putamen. In the caudate nucleus, there was an initial increase in the  $\text{BP}_{\text{ND}}$  values in the first four coronal planes in line with the highest level of  $\text{D}_{2/3}$  binding and DA concentration being localized in the head/mid-body, as reported earlier in *in vitro* autoradiographic studies (Camus et al. 1986; Kish et al. 1988). Thus, the overall decreasing gradient detected along the caudate nucleus is not necessarily linear. In the VST, a rather steep declining trend was seen. Previous post-mortem studies in humans have demonstrated that the distribution of striatal D2/3R is uniform both dorsoventrally and lateromedially (Hall et al. 1994; Piggott et al. 1999), whereas a rostrocaudally increasing gradient was detected in both the putamen and caudate nucleus (Piggott et al. 1999). These findings have been verified with the *in vivo* results conducted in pigs and monkeys (Rosa-Neto et al. 2004). There are no such studies using presynaptic markers such as DAT or DA synthesis (i.e.,  $^{18}\text{F}$ -DOPA), although regional changes in these markers have been the subject of numerous studies in PD. However, in one study, evidence was found for rostrocaudal gradients in [ $^3\text{H}$ ]dopamine uptake based on serial 2-mm sectioning in rats which detected a decreasing gradient in the dorsal–medial caudate nucleus along the AP axis (Deep et al. 1997). In the context of the functional association between pre- and post-synaptic markers, it might be speculated that the decreasing gradient of DA uptake in the rat striatum might be in agreement with the present findings. The volume of putamen is the largest of all striatal areas and its assessment is not substantially hampered by the limited number of coronal levels even with *in vitro* techniques, and it is not that vulnerable to PVE using PET. Unlike the putamen, PVE in the most caudal coronal planes of caudate nucleus, cannot be entirely excluded because the caudate nucleus narrows dramatically towards its tail. The  $\text{BP}_{\text{ND}}$  values of the VST were sampled from a total of only five coronal planes and again the presence of PVE may hamper the measurement, as the volume of the VST is very small. Thus, the observed gradient in the caudate nucleus and VST should be interpreted with caution. However, it is tempting to speculate that since endogenous dopamine has a higher affinity for the  $\text{D}_3$  type receptors, this could potentially lead to a larger underestimation of the overall D2/3R availability in  $\text{D}_3$  receptor-rich areas, such as the VST (Sokoloff et al. 1990; Gurevich and Joyce, 1999; Mawlawi et al. 2001). The relative amounts of  $\text{D}_3$  receptors are 33% in the nucleus accumbens, 26% in the ventral portions of the putamen, and 20% in the ventral portions of the caudate nucleus (Gurevich and Joyce, 1999), which seem to be in accordance with the descending trend seen in VST. In addition to the methodological differences between *in vivo* and *in vitro* techniques, the adult subjects in our study sample were young, in contrast with most of the subjects examined in post-mortem studies.



The striatum is a major part of the DA system's basal ganglia input and output and it can be divided into several anatomical and functional structures. The ventral regions play a key role in reward and reinforcement and are important in the development of addiction. Central areas are involved with cognitive functions such as working memory. The tasks mediated by the posterior areas are mainly related to motor activities (Haber et al. 2003). Dopamine D2/3R are expressed in the indirect pathway projecting to GPi and SNr via the STN (for review, see Gerfen et al. 1991;1992). In light of the present results, the higher  $BP_{ND}$  values detected in the posterior putamen emphasize the affiliation of this functional motor area with the indirect pathway. Because the striatum is connected with limbic, association, and motor cortical areas, processes associated with cognition and motor performance in both physiological and pathological states are characteristically manifested within this topography (DeLong, 1983; Evarts and Wise, 1984; Bäckman et al. 2000; Kaasinen and Rinne, 2002). Thus, the increasing gradient of D2/3R binding observed in the sensorimotor striatum could serve as a possible biomarker for neurodegenerative disorders, particularly those affecting the extrapyramidal system.

## 7. FUTURE DIRECTIONS

Study I demonstrated that the measurement of striatal and thalamic D2/3R binding was highly reliable, even when using high resolution techniques. The measurement of small striatal structures as VST was also equally reproducible. The statistical reconstruction of the HRRT was vulnerable to the bias inherent with low count statistics. However, utilizing a fixed number of counts did not improve the reproducibility or the reliability of the measurement. Although PSF reconstruction provided  $BP_{ND}$  estimates should be less contaminated by the PVE, the VAR and ICC values were somewhat inferior to the original non-PSF reconstruction. Ultimately, new, improved bias-free reconstruction schemes must be devised to remove the count statistics limitation in the HRRT studies. The manufacturing of the HRRT scanner has been closed down and the development of PET-scanners is focused more towards hybrid technology, such as combining PET and MRI modalities. The next generation HRRT is not available. Based on our results, high-resolution scanners are a very valuable tool in neuroimaging providing more accurate and reliable measurement of the DA neurotransmission. In the future, the development of brain dedicated high-resolution scanner is ultimately necessary.

Even though [ $^{11}C$ ]raclopride is ideal for imaging D2/3R rich areas such as striatum, it is considered to be non-ideal for quantifying D2/3R availability in cortex due to its moderate *in vivo* affinity and its relatively low signal-to-noise ratio (affinity compared with nonspecific binding) in low D2/3R density areas (Farde et al 1988). Despite these concerns, in study II, it was possible to achieve rather good reproducibility in cortex and thus to obtain supportive evidence that [ $^{11}C$ ]raclopride could be used also in cortical areas. However, displacement studies e.g. with haloperidol, will be needed to verify these findings. The ability to measure striatal and cortical DA transmission simultaneously would be highly beneficial offering more information about the connectivity of different functional and anatomical brain areas and their involvement in the neurobiology of both healthy and diseased brain.

Databases about the striatal and and extrastriatal dopamine D1, D2/3R bindings, DAT binding and endogenous dopamine synthesis rate measured in healthy subjects using different radiotracers have been constructed with less sensitive whole body PET scanners (Ito et al. 1999, 2008; Okubo et al. 1999). However, the gradients of the D2/3R binding have not been uniformly established in a living healthy human brain. Thus, the divergent rostrocaudal gradients in D2/3R binding observed in study III may impact the design and analyses of the future studies and serve as a possible database.

## 8. CONCLUSIONS

The major findings in this work are as follows:

- Test-retest reliability of dopamine D2/3R binding in the striatum and thalamus with [<sup>11</sup>C]raclopride is very good, even when using high-resolution techniques and longer scanning intervals.
- There was relatively low test-retest variability in the [<sup>11</sup>C]raclopride binding in the cortex, providing supportive evidence that with high-resolution techniques and protocol optimization extrastriatal DA transmission binding could be studied *in vivo* with [<sup>11</sup>C]raclopride PET.
- There are significant distinct gradients of dopamine D2/3R binding in the substriatal regions measured with [<sup>11</sup>C]raclopride and high-resolution PET that besides having a possible significant functional meaning, may also serve as a future database helping the differentiation of brain pathology.

## 9. ACKNOWLEDGEMENTS

As I look back over these past years, there are many people I would like to acknowledge. Their contribution, support and devotion towards my work have been indispensable.

I owe my biggest and heartfelt gratitude to my supervisor, Juha Rinne, whose ever-gentle and patient guidance have always been at my disposal. His positive attitude and drive have kept me going all these years, even at times when it all seemed impossible. His commitment towards my endeavours has been the key factor in the completion of this work, not to mention how privileged I have been to work under the guidance of such a great scientist with his level of knowledge in the field of neuroscience. I have been very fortunate to have Juha as my supervisor.

It is very hard to find words to thank my closest collaborator and dear friend Jarkko Johansson, whose input to this work has been priceless. Without your expertise, this work simply would not exist. Looking back from where we started, it has been an awesome journey. I also want to express my deepest gratitude to Juho Joutsa, who has what it seems like endless enthusiasm towards neuroscience. Thank you for your friendship and help during these years -and years to come, I hope.

I am very grateful to my co-authors, Terhi Tuokkola, Vesa Oikonen, Kjell Nägren, Matti Laine, Lars Nyberg, Lars Bäckman and Sargo Aalto. It has been a privilege to collaborate with you.

I would also like to thank the staff of Turku PET Centre and the Department of Clinical Physiology and Nuclear Medicine. The directors, Juhani Knuuti and Jaakko Hartiala, are thanked for giving me the opportunity to carry out my work in such great facilities with their superb scientific atmosphere. It has been a great pleasure to work alongside such skilled and nice people like Tarja Keskitalo, Minna Aatsinki, Hannele Lehtinen, Anne-Mari Jokinen, Eija Nirhamo, Tiina Santakivi, Sanna Suominen, Marjo Tähti and many others I have forgotten to name. Ulla Kulmala, Laura Kontto, Mirja Jyrkinen and Sinikka Lehtola are thanked for their kind help with the secretarial issues.

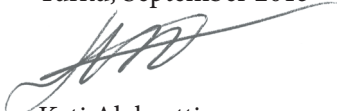
I wish to express my gratitude towards Jussi Hirvonen, Valtteri Kaasinen and Lauri Nummenmaa for their scientific guidance during these years and Marko Seppänen, Mika Teräs, Tuula Tolvanen and Virva Saunavaara for their help in resolving the many practical and technical issues. Rami Mikkola and Marko Tättäläinen are thanked for their expertise in IT related problems. I am grateful to the Department of Radiochemistry at Turku PET Centre and especially to Eveliina Arponen and Semi Helin for the synthesis of [ $^{11}\text{C}$ ]raclopride. I would also like to thank Esko Vanninen and Jesper Ekelund for using

their expertise in reviewing my thesis. Dr. Ewen MacDonald is acknowledged for the excellent and rapid grammatical review of my thesis.

My great fellow neuroscientists: Eero Rissanen, Lauri Tuominen, Anna Bruck, Nina Kemppainen, Laura Ekblad, Nora Lindgren, Henry Karlsson, Jetro Tuulari, Joonas Majuri, Henri Honka, Noora Scheinin, Pekka Jokinen, and Jere Virta; you are deeply appreciated for creating the inspiring scientific atmosphere in the Turku PET Centre and your excellent company outside the office. Alex Dickens, Susanne Vainio and Minna Yli-Karjanmaa are acknowledged from the preclinical division. Otto Waris and Anna Soveri are thanked for the ongoing and pleasant collaboration involving the Åbo Akademi, Department of Psychology. Jarmo Teuho, Pauliina Luoto, Jouni Tuisku and Jani Linden; I shared “the office” with you guys and I am forever indebted for your friendship, help and support. Joonas Eskelinen and Tiina Saanijoki: thank you for your friendship and support during these years. Finally I should mention the PET boys and girls and Team Rapa. I truly cherish the vivid conversations shared over a drink and the moments hurtling down the road.

I am very lucky to have such a big family and many dear friends. My parents Maire and Uolevi and my siblings Esko, Maarit, Suvi, Olli, Niklas and Aslak; thank you for your support and love. Tiina and Heli, it has been a pleasure to have you in our family. I am forever grateful to my oldest and dearest friends: Johanna, Hanna, Minna and Katja, you have been the ones keeping it real. Your presence in my life has truly been a gift. My closest friends from medschool, Paula, Sanni and Silva; you have given me so much joy during these past years and I am deeply grateful for your friendship and support. My extended Thai family: Inka, Mimmu, Teppo and many more, you have been amazing company every time the ground has started to burn under my feet. You have truly taken me into your hearts, as I have you. And Dan; you have been an example for me about the importance of pursuing your dreams and making them come true. I am forever indebted for your love, trust and support during all these years. You have been my bedrock, even in the darkest moments. Finally, I want to thank my mentor, ex-boss and colleague, Matti Kestilä. You have had such a strong influence on my path to this present moment, that there are no words to describe it. I can only say that without your belief in me, I wouldn't be here. You have taught me everything about elegance, grace and mercy.

Turku, September 2015



Kati Alakurtti

## 10. REFERENCES

- Abi-Dargham, A., Gil, R., Krystal, J., Baldwin, R.M., Seibyl, J.P., Bowers, M., van Dyck, D.S., Innis, R.B., Laruelle, M., 1998. Increased striatal dopamine transmission in schizophrenia: confirmation in a second cohort. *Am J Psychiatry* 155, 761–767.
- Antonini, A., Leenders, K.L., 1993. Dopamine D2 receptors in normal human brain: effect of age measured by positron emission tomography (PET) and [<sup>11</sup>C]-raclopride. *Ann. N. Y. Acad. Sci.* 695, 81–85.
- Antonini, A., Leenders, K.L., Vontobel, P., Maguire, R.P., Missimer, J., Psylla, M., Günther, I., 1997. Complementary PET studies of striatal neuronal function in the differential diagnosis between multiple system atrophy and Parkinson's disease. *Brain* 120 (Pt 12), 2187–2195.
- Belin, D., Everitt, B.J., 2008. Cocaine seeking habits depend upon dopamine-dependent serial connectivity linking the ventral with the dorsal striatum. *Neuron* 57, 432–441.
- Beaulieu, J.-M., Gainetdinov, R.R., 2011. The Physiology, Signaling, and Pharmacology of Dopamine Receptors. *Pharmacol Rev* 63, 182–217.
- Breier, A., Adler, C.M., Weisenfeld, N., Su, T.P., Elman, I., Picken, L., Malhotra, A.K., Pickar, D., 1998. Effects of NMDA antagonism on striatal dopamine release in healthy subjects: application of a novel PET approach. *Synapse* 29, 142–147.
- Brooks, D.J., Ibanez, V., Sawle, G.V., Playford, E.D., Quinn, N., Mathias, C.J., Lees, A.J., Marsden, C.D., Bannister, R., Frackowiak, R.S., 1992. Striatal D2 receptor status in patients with Parkinson's disease, striatonigral degeneration, and progressive supranuclear palsy, measured with <sup>11</sup>C-raclopride and positron emission tomography. *Ann. Neurol.* 31, 184–192.
- Brücke, T., Asenbaum, S., Pirker, W., Djamshidian, S., Wenger, S., Wöber, C., Müller, C., Podreka, I., 1997. Measurement of the dopaminergic degeneration in Parkinson's disease with [<sup>123</sup>I] beta-CIT and SPECT. Correlation with clinical findings and comparison with multiple system atrophy and progressive supranuclear palsy. *J. Neural Transm. Suppl.* 50, 9–24.
- Bäckman, L., Nyberg, L., Soveri, A., Johansson, J., Andersson, M., Dahlin, E., et al. 2011. Effects of working-memory training on striatal dopamine release. *Science* 333, 718.
- Bäckman, L., Nyberg, L., Lindenberg, U., Li, S.-C., Farde, L., 2006. The correlative triad among aging, dopamine, and cognition: current status and future prospects. *Neurosci. Biobehav. Rev.* 30, 791–807.
- Bäckman, L., Ginovart, N., Dixon, R.A., Wahlin, T.B., Wahlin, A., Halldin, C., Farde, L., 2000. Age-related cognitive deficits mediated by changes in the striatal dopamine system. *Am. J. Psychiatry* 157, 635–637.
- Camardese, G., Di Giuda, D., Di Nicola, M., Cocciolillo, F., Giordano, A., Janiri, L., Guglielmo, R., 2014. Imaging studies on dopamine transporter and depression: a review of literature and suggestions for future research. *J Psychiatr Res* 51, 7–18.
- Camus, A., Javoy-Agid, F., Dubois, A., Scatton, B., 1986. Autoradiographic localization and quantification of dopamine D2 receptors in normal human brain with [<sup>3</sup>H]Nn-propylnorapomorphine. *Brain Res.* 375, 135–149.
- Carson, R.E., Breier, A., de Bartolomeis, A., Saunders, R.C., Su, T.P., Schmall, B., et al. 1997. Quantification of amphetamine-induced changes in [<sup>11</sup>C]raclopride binding with continuous infusion. *J. Cereb. Blood Flow Metab.* 17, 437–447.
- Comtat, C., Bataille, F., Michel, C., Jones, J.P., Sibomana, M., Janeiro, L., Trebossen, R., 2004. OSEM-3D reconstruction strategies for the ECAT HRRT. *Nuclear Science Symposium Conference Record, 2004 IEEE*, vol. 6, pp. 3492–3496.
- Comtat, C., Sureau, F.C., Sibomana, M., Hong, I.K., Sjöholm, N., Trebossen, R., 2008. Image based resolution modeling for the HRRT OSEM reconstructions software. *Nuclear Science Symposium Conference Record, 2008: NSS '08. IEEE*, pp. 4120–4123.
- Deep, P., Kuwabara, H., Gjedde, A., Cumming, P., 1997. The kinetic behaviour of [<sup>3</sup>H]DOPA in living rat brain investigated by compartmental modelling of static autoradiograms. *J. Neurosci. Methods* 78, 157–168.
- De Jong, H.W.A.M., van Velden, F.H.P., Kloet, R.W., Buijs, F.L., Boellaard, R., Lammertsma, A.A., 2007. Performance evaluation of the ECAT HRRT: an LSO-LYSO double layer high resolution, high sensitivity scanner. *Phys Med Biol* 52, 1505–1526.
- DeLong, M.R., 1983. The neurophysiologic basis of abnormal movements in basal ganglia disorders. *Neurobehav. Toxicol. Teratol.* 5, 611–616.
- Dewey, S.L., Brodie, J.D., Fowler, J.S., MacGregor, R.R., Schlyer, D.J., King, P.T., Alexoff, N.D., Shiue, C.Y., Wolf, A.P., 1990. Positron emission tomography (PET) studies of dopaminergic/cholinergic interactions in the baboon brain. *Synapse* 6, 321–327.
- Dewey, S.L., Logan, J., Wolf, A.P., Brodie, J.D., Angrist, B., Fowler, J.S., Volkow, N.D., 1991. Amphetamine

- induced decreases in (18F)-N-methylspiroperidol binding in the baboon brain using positron emission tomography (PET). *Synapse* 7, 324–327.
- Dewey, S.L., Smith, G.S., Logan, J., Brodie, J.D., Simkowitz, P., MacGregor, R.R., Fowler, J.S., Volkow, N.D., Wolf, A.P., 1993. Effects of central cholinergic blockade on striatal dopamine release measured with positron emission tomography in normal human subjects. *Proc. Natl. Acad. Sci. U.S.A.* 90, 11816–11820.
- Dickson, D.W., 2012. Parkinson's disease and parkinsonism: neuropathology. *Cold Spring Harb Perspect Med* 2.
- Dreve DN et al., Cortical surface-based analysis reduces bias and variance in kinetic modeling of brain PET data. *Neuroimage*. 2014 May 15;92:225-36.
- Drevets, W.C., Price, J.C., Kupfer, D.J., Kinahan, P.E., Lopresti, B., Holt, D., et al. 1999. PET measures of amphetamine-induced dopamine release in ventral versus dorsal striatum. *Neuropsychopharmacology* 21, 694–709.
- Egerton, A., Mehta, M.A., Montgomery, A.J., Lappin, J.M., Howes, O.D., Reeves, S.J., Cunningham, V.J., Grasby, P.M., 2009. The dopaminergic basis of human behaviors: A review of molecular imaging studies. *Neuroscience & Biobehavioral Reviews* 33, 1109–1132.
- Evarts, E.V., Wise, S.P., 1984. Basal ganglia outputs and motor control. *CIBA Found. Symp.* 107, 83–102.
- Farde, L., Ehrin, E., Eriksson, L., Greitz, T., Hall, H., Hedström, C.G., et al. 1985. Substituted benzamides as ligands for visualization of dopamine receptor binding in the human brain by positron emission tomography. *Proc. Natl. Acad. Sci. U.S.A.* 82, 3863–3867.
- Farde, L., Pauli, S., Hall, H., Eriksson, L., Halldin, C., Högberg, T., et al. 1988. Stereoselective binding of <sup>11</sup>C-raclopride in living human brain--a search for extrastriatal central D2-dopamine receptors by PET. *Psychopharmacology (Berl.)* 94, 471–478.
- Gerfen, C.R., McGinty, J.F., Young, W.S., 3rd, 1991. Dopamine differentially regulates dynorphin, substance P, and enkephalin expression in striatal neurons: in situ hybridization histochemical analysis. *J. Neurosci.* 11, 1016–1031.
- Gerfen, C.R., 1992. The neostriatal mosaic: multiple levels of compartmental organization. *Trends Neurosci.* 15, 133–139.
- Ghaemi, M., Hilker, R., Rudolf, J., Sobesky, J., Heiss, W.-D., 2002. Differentiating multiple system atrophy from Parkinson's disease: contribution of striatal and midbrain MRI volumetry and multi-tracer PET imaging. *J. Neurol. Neurosurg. Psychiatry* 73, 517–523.
- Guillin, O., Abi-Dargham, A., Laruelle, M., 2007. Neurobiology of dopamine in schizophrenia. *Int. Rev. Neurobiol.* 78, 1–39.
- Gurevich, E.V., Joyce, J.N., 1999. Distribution of dopamine D3 receptor expressing neurons in the human forebrain: comparison with D2 receptor expressing neurons. *Neuropsychopharmacology* 20, 60–80.
- Gunn, R.N., Lammertsma, A.A., Hume, S.P., Cunningham, V.J., 1997. Parametric imaging of ligand-receptor binding in PET using a simplified reference region model. *Neuroimage* 6, 279–287.
- Haber, S.N., 2003. The primate basal ganglia: parallel and integrative networks. *J. Chem. Neuroanat.* 26, 317–330.
- Hall, H., Sedvall, G., Magnusson, O., Kopp, J., Halldin, C., Farde, L., 1994. Distribution of D1- and D2-dopamine receptors, and dopamine and its metabolites in the human brain. *Neuropsychopharmacology* 11, 245–256.
- Hall, H., Köhler, C., Gawell, L., Farde, L., Sedvall, G., 1988. Raclopride, a new selective ligand for the dopamine-D2 receptors. *Prog. Neuropsychopharmacol. Biol. Psychiatry* 12, 559–568.
- Hall, H., Farde, L., Halldin, C., Hurd, Y.L., Pauli, S., Sedvall, G., 1996. Autoradiographic localization of extrastriatal D2-dopamine receptors in the human brain using [<sup>125</sup>I]epidepride. *Synapse* 23, 115–123.
- Halldin, C., Farde, L., Högberg, T., Mohell, N., Hall, H., Suhara, T., et al. 1995. Carbon-11-FLB 457: a radioligand for extrastriatal D2 dopamine receptors. *J. Nucl. Med.* 36, 1275–1281.
- Hietala, J., Nägren, K., Lehtikoinen, P., Ruotsalainen, U., Syvälahti, E., 1999. Measurement of striatal D2 dopamine receptor density and affinity with [<sup>11</sup>C]-raclopride in vivo: a test-retest analysis. *J. Cereb. Blood Flow Metab.* 19, 210–217.
- Hirvonen, J., Aalto, S., Lumme, V., Nägren, K., Kajander, J., Vilkmann, H., et al. 2003. Measurement of striatal and thalamic dopamine D2 receptor binding with <sup>11</sup>C-raclopride. *Nucl Med Commun* 24, 1207–1214.
- Innis, R.B., Cunningham, V.J., Delforge, J., Fujita, M., Gjedde, A., Gunn, R.N., et al. 2007. Consensus nomenclature for in vivo imaging of reversibly binding radioligands. *J. Cereb. Blood Flow Metab.* 27, 1533–1539.
- Ito, H., Okubo, Y., Halldin, C., Farde, L., 1999. Mapping of central D2 dopamine receptors in man using [<sup>11</sup>C]raclopride: PET with anatomic standardization technique. *Neuroimage* 9, 235–242. doi:10.1006/nimg.1998.0401
- Ito, H., Takahashi, H., Arakawa, R., Takano, H., Suhara, T., 2008. Normal database of dopaminergic neurotransmission system in human brain measured

- by positron emission tomography. *Neuroimage* 39, 555–565. doi:10.1016/j.neuroimage.2007.09.011
- Joel, D., Weiner, I., 2000. The connections of the dopaminergic system with the striatum in rats and primates: an analysis with respect to the functional and compartmental organization of the striatum. *Neuroscience* 96, 451–474.
- Johansson J, Oikonen V, Teras M (2007) Quantitative brain imaging using the new, fast iterative histogram-mode reconstruction for the HRRT PET scanner. *IEEE Nucl Sci Conf R* 2007 5:3463--7
- Jonasson, L.S., Axelsson, J., Riklund, K., Braver, T.S., Ogren, M., Bäckman, L., Nyberg, L., 2014. Dopamine release in nucleus accumbens during rewarded task switching measured by [(11)C]raclopride. *Neuroimage*.
- Joyce, J.N., Myers, A.J., Gurevich, E., 1998. Dopamine D2 receptor bands in normal human temporal cortex are absent in Alzheimer's disease. *Brain Res.* 784, 7–17.
- Kaasinen, V., Rinne, J.O., 2002. Functional imaging studies of dopamine system and cognition in normal aging and Parkinson's disease. *Neurosci. Biobehav. Rev.* 26, 785–793.
- Kim, J.-H., Son, Y.-D., Kim, H.-K., Lee, S.-Y., Cho, S.-E., Kim, Y.-B., Cho, Z.-H., 2011. Effects of age on dopamine D(2) receptor availability in striatal subdivisions: a high-resolution positron emission tomography study. *Eur. Neuropsychopharmacol.* 21, 885–891.
- Kish, S.J., Shannak, K., Hornykiewicz, O., 1988. Uneven pattern of dopamine loss in the striatum of patients with idiopathic Parkinson's disease. Pathophysiologic and clinical implications. *N. Engl. J. Med.* 318, 876–880.
- Kuepper, R., Skinbjerg, M., Abi-Dargham, A., 2012. The dopamine dysfunction in schizophrenia revisited: new insights into topography and course. *Handb. Exp. Pharmacol.* 1–26.
- Lammertsma, A.A., Hume, S.P., 1996. Simplified reference tissue model for PET receptor studies. *Neuroimage* 4, 153–158.
- Laruelle, M., 2000. Imaging synaptic neurotransmission with in vivo binding competition techniques: a critical review. *J. Cereb. Blood Flow Metab.* 20, 423–451.
- Laruelle, M., Slifstein, M., Huang, Y., 2003. Relationships between radiotracer properties and image quality in molecular imaging of the brain with positron emission tomography. *Mol Imaging Biol* 5, 363–375.
- Leroy C, Comtat C, Trébossen R, Syrota A, Martinot J-L, Ribeiro M-J (2007) Assessment of 11C-PE2I binding to the neuronal dopamine transporter in humans with the high-spatial-resolution PET scanner HRRT. *J Nucl Med* 48:538–546
- Logan, J., Dewey, S.L., Wolf, A.P., Fowler, J.S., Brodie, J.D., Angrist, B., Volkow, N.D., Gatley, S.J., 1991. Effects of endogenous dopamine on measures of [18F]N-methylspiperidol binding in the basal ganglia: comparison of simulations and experimental results from PET studies in baboons. *Synapse* 9, 195–207.
- Mintun, M.A., Raichle, M.E., Kilbourn, M.R., Wooten, G.F., Welch, M.J., 1984. A quantitative model for the in vivo assessment of drug binding sites with positron emission tomography. *Ann. Neurol.* 15, 217–227.
- Missale, C., Nash, S.R., Robinson, S.W., Jaber, M., Caron, M.G., 1998. Dopamine receptors: from structure to function. *Physiol. Rev.* 78, 189–225.
- Martinez, D., Kim, J.-H., Krystal, J., Abi-Dargham, A., 2007. Imaging the neurochemistry of alcohol and substance abuse. *Neuroimaging Clin. N. Am.* 17, 539–555, x.
- Martinez, D., Slifstein, M., Broft, A., Mawlawi, O., Hwang, D.-R., Huang, Y., et al. 2003. Imaging human mesolimbic dopamine transmission with positron emission tomography. Part II: amphetamine-induced dopamine release in the functional subdivisions of the striatum. *J. Cereb. Blood Flow Metab.* 23, 285–300.
- Mawlawi, O., Martinez, D., Slifstein, M., Broft, A., Chatterjee, R., Hwang, D.R., et al. 2001. Imaging human mesolimbic dopamine transmission with positron emission tomography: I. Accuracy and precision of D(2) receptor parameter measurements in ventral striatum. *J. Cereb. Blood Flow Metab.* 21, 1034–1057.
- Meisenzahl, E. M., G. J. Schmitt, J. Scheuerecker, ja H.-J. Möller. "The role of dopamine for the pathophysiology of schizophrenia". *International Review of Psychiatry* 19, 2007; 4:337–45.
- Mourik JEM, Lubberink M, van Velden FHP, Kloet RW, van Berckel BNM, Lammertsma AA, Boellaard R (2010) In vivo validation of reconstruction-based resolution recovery for human brain studies. *J Cereb Blood Flow Metab* 30:381–389
- Mukherjee, J., Christian, B.T., Dunigan, K.A., Shi, B., Narayanan, T.K., Satter, M., et al. 2002. Brain imaging of 18F-fallypride in normal volunteers: blood analysis, distribution, test-retest studies, and preliminary assessment of sensitivity to aging effects on dopamine D-2/D-3 receptors. *Synapse* 46, 170–188.
- Narendran, R., Hwang, D.-R., Slifstein, M., Talbot, P.S., Erritzoe, D., Huang, Y., Cooper, T.B., Martinez, D., Kegeles, L.S., Abi-Dargham, A., Laruelle, M., 2004. In vivo vulnerability to competition by endogenous dopamine: comparison of the D2 receptor agonist



- radiotracer (-)-N-[11C]propyl-norapomorphine ([11C]NPA) with the D2 receptor antagonist radiotracer [11C]-raclopride. *Synapse* 52, 188–208.
- Narendran, R., Frankle, W.G., Mason, N.S., Rabiner, E.A., Gunn, R.N., Searle, G.E., Vora, S., Litschge, M., Kendro, S., Cooper, T.B., Mathis, C.A., Laruelle, M., 2009. Positron emission tomography imaging of amphetamine-induced dopamine release in the human cortex: a comparative evaluation of the high affinity dopamine D2/3 radiotracers [11C]FLB 457 and [11C]fallypride. *Synapse* 63, 447–461.
- Nieoullon, A., 2002. Dopamine and the regulation of cognition and attention. *Prog. Neurobiol.* 67, 53–83.
- Okubo, Y., Olsson, H., Ito, H., Lofti, M., Suhara, T., Halldin, C., Farde, L., 1999. PET mapping of extrastriatal D2-like dopamine receptors in the human brain using an anatomic standardization technique and [11C]FLB 457. *Neuroimage* 10, 666–674. doi:10.1006/nimg.1999.0502
- Olsson, H., Halldin, C., Farde, L., 2004. Differentiation of extrastriatal dopamine D2 receptor density and affinity in the human brain using PET. *Neuroimage* 22, 794–803.
- Parent, A., Hazrati, L.N., 1995. Functional anatomy of the basal ganglia. I. The cortico-basal ganglia-thalamo-cortical loop. *Brain Res. Brain Res. Rev.* 20, 91–127.
- Pavese, N., Andrews, T.C., Brooks, D.J., Ho, A.K., Rosser, A.E., Barker, R.A., Robbins, T.W., Sahakian, B.J., Dunnett, S.B., Piccini, P., 2003. Progressive striatal and cortical dopamine receptor dysfunction in Huntington's disease: a PET study. *Brain* 126, 1127–1135.
- Piccini, P., Pavese, N., Brooks, D.J., 2003. Endogenous dopamine release after pharmacological challenges in Parkinson's disease. *Ann. Neurol.* 53, 647–653.
- Pierce, R.C., Kumaresan, V., 2006. The mesolimbic dopamine system: the final common pathway for the reinforcing effect of drugs of abuse? *Neurosci Biobehav Rev* 30, 215–238.
- Piggott, M.A., Marshall, E.F., Thomas, N., Lloyd, S., Court, J.A., Jaros, E., Costa, D., Perry, R.H., Perry, E.K., 1999. Dopaminergic activities in the human striatum: rostrocaudal gradients of uptake sites and of D1 and D2 but not of D3 receptor binding or dopamine. *Neuroscience* 90, 433–445.
- Planeta-Wilson B, Yan J, Mulnix T, Carson RE (2008) Quantitative accuracy of HRRT list-mode constructions: effect of low statistics. *IEEE Nucl Sci Conf R* 2008, 5121–24
- Politis, M., Pavese, N., Tai, Y.F., Kiferle, L., Mason, S.L., Brooks, D.J., et al. 2011. Microglial activation in regions related to cognitive function predicts disease onset in Huntington's disease: a multimodal imaging study. *Hum Brain Mapp* 32, 258–270.
- Ribeiro, M.-J., Thobois, S., Lohmann, E., du Montcel, S.T., Lesage, S., Pelissolo, A., et al. 2009. A multitracers dopaminergic PET study of young-onset parkinsonian patients with and without parkin gene mutations. *J. Nucl. Med.* 50, 1244–1250.
- Rinne, J.O., Laihinen, A., Lönnberg, P., Marjamäki, P., Rinne, U.K., 1991. A post-mortem study on striatal dopamine receptors in Parkinson's disease. *Brain Res.* 556, 117–122.
- Rinne, J.O., Hietala, J., Ruotsalainen, U., Säkö, E., Laihinen, A., Nägren, K., Lehtikoinen, P., Oikonen, V., Syvälahti, E., 1993. Decrease in human striatal dopamine D2 receptor density with age: a PET study with [11C]raclopride. *J. Cereb. Blood Flow Metab.* 13, 310–314.
- Rosa-Neto, P., Doudet, D.J., Cumming, P., 2004. Gradients of dopamine D1- and D2/3-binding sites in the basal ganglia of pig and monkey measured by PET. *NeuroImage* 22, 1076–1083.
- Ross, S.B., Jackson, D.M., 1989. Kinetic properties of the in vivo accumulation of 3H-(-)-N-n-propyl-norapomorphine in mouse brain. *Naunyn Schmiedeberg's Arch. Pharmacol.* 340, 13–20.
- Sawamoto, N., Piccini, P., Hotton, G., Pavese, N., Thielemans, K., Brooks, D.J., 2008. Cognitive deficits and striato-frontal dopamine release in Parkinson's disease. *Brain* 131, 1294–1302.
- Seeman, P., Bzowej, N.H., Guan, H.C., Bergeron, C., Becker, L.E., Reynolds, G.P., Bird, E.D., Riederer, P., Jellinger, K., Watanabe, S., 1987. Human brain dopamine receptors in children and aging adults. *Synapse* 1, 399–404.
- Seeman, P., Guan, H.C., Niznik, H.B., 1989. Endogenous dopamine lowers the dopamine D2 receptor density as measured by [3H]raclopride: implications for positron emission tomography of the human brain. *Synapse* 3, 96–97.
- Shotbolt, P., Tziortzi, A.C., Searle, G.E., Colasanti, A., van der Aart, J., Abanades, S., Plisson, C., Miller, S.R., Huiban, M., Beaver, J.D., Gunn, R.N., Laruelle, M., Rabiner, E.A., 2012. Within-subject comparison of [(11)C]-(+)-PHNO and [(11)C]raclopride sensitivity to acute amphetamine challenge in healthy humans. *J. Cereb. Blood Flow Metab.* 32, 127–136
- Slifstein, M., Hwang, D.-R., Huang, Y., Guo, N., Sudo, Y., Narendran, R., Talbot, P., Laruelle, M., 2004. In vivo affinity of [18F]fallypride for striatal and extrastriatal dopamine D2 receptors in nonhuman primates. *Psychopharmacology (Berl.)* 175, 274–286.
- Sokoloff, P., Giros, B., Martres, M.P., Bouthenet, M.L., Schwartz, J.C., 1990. Molecular cloning and characterization of a novel dopamine receptor (D3) as a target for neuroleptics. *Nature* 347, 146–151.

- Sossi V, de Jong H, Barker W, Bloomfield P, Burbar Z, Camborde M, Comtat C, Eriksson L, Houle S, Keator D, Knöös C, Kraiss R, Lammertsma A, Rahmim A, Sibomana M, Teräs M, Thompson C, Trebossen R, Votaw J, Walker M, Wienhard K, Wong D (2005) The second generation HRRT: a multi-centre scanner performance investigation. *Conf Rec 2005 IEEE Nucl Sci Symp Med Imaging Conf (Puerto Rico)* 4:2195–2199
- Stokes, P.R.A., Egerton, A., Watson, B., Reid, A., Breen, G., Lingford-Hughes, A., et al. 2010. Significant decreases in frontal and temporal [11C]-raclopride binding after THC challenge. *Neuroimage* 52, 1521–1527.
- Suhara, T., Sudo, Y., Okauchi, T., Maeda, J., Kawabe, K., Suzuki, K., et al. 1999. Extrastriatal dopamine D2 receptor density and affinity in the human brain measured by 3D PET. *Int. J. Neuropsychopharmacol.* 2, 73–82.
- Sureau FC, Reader AJ, Comtat C, Leroy C, Ribeiro M-J, Buvat I, Trébossen R (2008) Impact of image-space resolution modeling for studies with the high-resolution research tomograph. *J Nucl Med* 49:1000–8
- Turkington, T.G., 2001. Introduction to PET instrumentation. *J Nucl Med Technol* 29, 4–11.
- Varrone A, Sjöholm N, Eriksson L, Gulyás B, Halldin C, Farde L (2009) Advancement in PET quantification using 3D-OP-OSEM point spread function reconstruction with the HRRT. *Eur J Nucl Med Mol Imaging*, 10:1639–50
- van Velden FHP, Kloet RW, van Berckel BNM, Wolfensberger SPA, Lammertsma AA, Boellaard R (2008) Comparison of 3D-OP-OSEM and 3D-FBP reconstruction algorithms for High-Resolution Research Tomograph studies: effects of randoms estimation methods. *Phys Med Biol* 53:3217–30
- Verel, I., Visser, G.W.M., van Dongen, G.A., 2005. The promise of immuno-PET in radioimmunotherapy. *J. Nucl. Med.* 46 Suppl 1, 164S–71S.
- Vilkman, H., Kajander, J., Nägren, K., Oikonen, V., Syvälahti, E., Hietala, J., 2000. Measurement of extrastriatal D2-like receptor binding with [11C] FLB 457--a test-retest analysis. *Eur J Nucl Med* 27, 1666–1673.
- Volkow, N.D., Fowler, J.S., Wang, G.J., Hitzemann, R., Logan, J., Schlyer, D.J., Dewey, S.L., Wolf, A.P., 1993b. Decreased dopamine D2 receptor availability is associated with reduced frontal metabolism in cocaine abusers. *Synapse* 14, 169–177.
- Volkow, N.D., Gur, R.C., Wang, G.J., Fowler, J.S., Moberg, P.J., Ding, Y.S., Hitzemann, R., S Byars LG, Sibomana M, Burbar Z, Jones J, Panin V, Barker WC, Liow J-S, Carson RE, Michel C (2005) Variance reduction on randoms from coincidence histograms for the HRRT. *IEEE Nucl Sci Conf R* 2005:2622–6
- Volkow ND, Fowler JS, Wang GJ, Dewey SL, Schlyer D, MacGregor R, Logan J, Alexoff D, Shea C, Hitzemann R (1993) Reproducibility of repeated measures of carbon-11-raclopride binding in the human brain. *J Nucl Med* 34:609--13
- Volkow ND, Smith, G., Logan, J., 1998. Association between decline in brain dopamine activity with age and cognitive and motor impairment in healthy individuals. *Am. J. Psychiatry* 155, 344–349.
- Volkow, N.D., Wang, G.J., Fowler, J.S., Logan, J., Gatley, S.J., Gifford, A., Hitzemann, R., Ding, Y.S., Pappas, N., 1999. Prediction of reinforcing responses to psychostimulants in humans by brain dopamine D2 receptor levels. *Am. J. Psychiatry* 156, 1440–1443
- Volkow, N.D., Wang, G.-J., Newcorn, J.H., Kollins, S.H., Wigal, T.L., Telang, F., Fowler, J.S., Goldstein, R.Z., Klein, N., Logan, J., Wong, C., Swanson, J.M., 2011. Motivation deficit in ADHD is associated with dysfunction of the dopamine reward pathway. *Mol. Psychiatry* 16, 1147–1154.
- Volkow, N.D., Wang, G.-J., Fowler, J.S., Tomasi, D., Telang, F., 2011. Addiction: beyond dopamine reward circuitry. *Proc. Natl. Acad. Sci. U.S.A.* 108, 15037–15042.
- Volkow, N.D., Wang, G.J., Fowler, J.S., Logan, J., Schlyer, D., Hitzemann, R., Lieberman, J., Angrist, B., Pappas, N., MacGregor, R., 1994. Imaging endogenous dopamine competition with [11C]raclopride in the human brain. *Synapse* 16, 255–262.
- Walker MD, Julyan PJ, Talbot PS, Jones T, Matthews JC (2009) Bias in iterative reconstruction of low-statistics PET data: benefits of a resolution model. *IEEE Nucl Sci Conf R* 2009, 2857–63
- Watabe, H., Endres, C.J., Breier, A., Schmall, B., Eckelman, W.C., Carson, R.E., 2000. Measurement of dopamine release with continuous infusion of [11C]raclopride: optimization and signal-to-noise considerations. *J. Nucl. Med.* 41, 522–530.
- Wong, D.F., Brasić, J.R., Singer, H.S., Schretlen, D.J., Kuwabara, H., Zhou, Y., Nandi, A., Maris, M.A., Alexander, M., Ye, W., Rousset, O., Kumar, A., Szabo, Z., Gjedde, A., Grace, A.A., 2008. Mechanisms of dopaminergic and serotonergic neurotransmission in Tourette syndrome: clues from an in vivo neurochemistry study with PET. *Neuropsychopharmacology* 33, 1239–1251.
- Young, L.T., Wong, D.F., Goldman, S., Minkin, E., Chen, C., Matsumura, K., Scheffel, U., Wagner, H.N., 1991. Effects of endogenous dopamine on kinetics of [3H] N-methylspiperone and [3H]raclopride binding in the rat brain. *Synapse* 9, 188–194.